KHAZAR UNIVERSITY

Faculty: Graduate School of Science, Art and Technology
Department: Electronics, Telecommunications and Radio Engineering
Specialty: Electronics and Automation

MASTER THESIS

Theme: Visualizing the signal of the metal detector and increasing the efficiency of the search

Master Student: Kamran Aliyev
Supervisor: Ph.D. Nuru Arab Safarov

BAKU – 2021

ABSTRACT

In this thesis, the design and analysis of multi-frequency metal detectors that allow the classification of metallic objects is explained. The working method of the designed detector is similar to the continuous wave metal detector, but it works in the range of 1 kHz to 100 kHz instead of a single frequency. As the amount of distinctive information from the target object increases, classification becomes easier.

In the theoretical analysis part of the thesis, the working principles of metal detectors are explained. In addition, the working methods of pulse induction metal detectors and continuous wave metal detectors are explained in detail. A basic induction circuit model has been created to perform electromagnetic analysis in frequency space. Since it works at low frequencies, the equations are made easier and their solutions are made by using the quasi-static approach.

In the hardware design part, the appropriate inductance value of the coils in the 1 kHz - 100 kHz band range is calculated. The induction reset of the double-D coil, which is suitable for the design, is done. Afterwards, it is isolated from capacitive effects and external EM noises with metallic fabric. The weak signals received with the phase inverting differential amplifier are amplified.

In the data analysis part, a remote computer-controlled test setup was set up in the laboratory environment. Signal generator and oscilloscope were controlled via computer with LabVIEW® program. The phase and amplitude data of the signal received with the LabVIEW® interface are recorded in the file. With the MATLAB® program, coherent and quadrature signal segments were created from the phase and amplitude data. The graphs were drawn according to the phase, amplitude, coherent and quadrature data of the signal taken from the test objects, and their analyzes were made.

1. INTRODUCTION

Metal detectors are devices used to detect metallic objects. It is used in many areas today. Military purpose metal detectors are used to detect dangerous objects such as mines, unexploded ammunition and handmade explosives. Scientific and commercial metal detectors are used in geophysical investigations, food industry, security systems and treasure searches.

The first metal detector definition was introduced by Saxby [1] in 1868. However, this detector only detected magnetic metals. This forms the basis of passive metal detectors. The first metal detector that detects all metallic objects was designed by Hughes in 1872 [1].

Metal detectors with many different operating techniques have been developed since the day it was first designed. While geophysical studies show 100 meters below the ground, it is expected to find small pieces of metal at close range in the food and pharmaceutical industry. Therefore, its design varies according to different purposes.

Advanced metal detectors can provide many information such as the type and depth of the metal as well as detecting the metal. According to the working methods, it works in time space or frequency space. They have advantages and disadvantages over each other. While the classification of metals in pulse induction metal detectors operating in time space is complex, it is easier to classify ferromagnetic and non-ferromagnetic metals in continuous wave metal detectors operating in frequency space. In the researches, it has been observed that metallic objects produce characteristic signs in the frequency domain according to their magnetic properties and physical properties [2]. By using these characteristics, false alarms in detectors are reduced.

With the subject of the thesis "design and analysis of multi-frequency metal detector", a continuous wave metal detector operating in a frequency range of

1 kHz-100 kHz is designed. Electromagnetic responses of metallic objects have been analyzed. A proposal has been made for the classification of metals.

1.1 Types of Metal Detector

1.1.1 Detectors for military purposes

Mined land clearance is a major problem for many countries. War-era mines, unexploded munitions and handmade explosives buried by terrorist groups pose a life-threatening hazard for people. These lands are cleaned by using military metal detectors. Figure 1.1 gives an example of portable mine detectors.

Figure 1.1 : a) Vallon brand metal detector [21] b) ETMTS-2 GPR and Metal detector [22].

International and national centers have been set up to clean mines and buried explosives. Geneva International Humanitarian Mine Clearance Center

(GICHD) and national Mine Action Centers (MAC) in countries such as Afghanistan and Cambodia guide countries in clearing dangerous explosives.

Mines are widely used by terrorist groups because of their low cost, difficulty to detect and find. Antipersonnel mines are difficult to detect since they contain too little metal. This is due to the low metal density and mineral structure in the soil. It may cause false detection by producing signs at the same or higher level with the explosive object. Inaccurate detections cause the detector's performance to degrade and it takes a long time to clear mined areas. In order to prevent false alarm rates of metal detectors in military use, advanced metal detector technologies are used [1].

1.1.2 Detectors for commercial purposes

Treasure detectors are detectors developed to find precious coins and metals from ancient times. These detectors distinguish materially valuable metals such as silver and gold. Figure 1.2 shows an example metal detector.

Figure 1.2 : Garrett brand treasure detector [23].

There are treasure detectors with large search coils for detecting metals in deep distances. Commercially Minelab, Fisher, Garrett etc. There are many brands.

Security door detectors are used extensively today to provide safe passage to buildings or environments. There are walk-through and handheld versions for object search. It has become important to prevent malicious people from wandering in crowded places with dangerous objects such as guns and knives. It is used extensively in shopping centers and business entrances.

An example of this type of detector is given in Figure 1.3. In geophysical studies, magnetometer, which is a type of metal detector, is used to extract the magnetic field line characteristic of the ground. It is used in metallic examination and mapping studies of the earth.

Figure 1.3: Metal detectors in security systems [24].

Metal detector technology is used in non-destructive tests (Non-Destructive Testing, NdT). It is a test process that is carried out without damaging the entire material to be examined. It is used to analyze metallic materials such as bars and plates. It detects invisible discontinuities and deteriorations in the material [3]. It is a test cycle that is done without harming the whole material to be inspected. It is utilized to investigate metallic materials like bars and plates.

1.2 Purpose and Content of the Thesis Study

The biggest problem encountered with metal detectors is high false alarm rates. Many metal parts found in nature cause false alarms. Even if there is no metallic object in the soil, metal detectors can detect according to the iron content in the soil. Iron content, especially in soils in the volcanic volcano region, reacts with a greater amplitude than many anti-personnel mines. Therefore, ground compensation methods, in which the ground effect is neglected, is an indispensable feature for metal detectors. Ground compensation can be done with continuous wave metal detectors operating in frequency domain. In addition, it is possible to distinguish the objects with these detectors. In basic principle, each metallic object is expected to respond differently as its frequency changes. Therefore, multi-frequency metal detectors can reduce false alarms [2,6]. With these properties, the characteristics of the objects can be deduced. Multi-frequency metal detectors can provide much more information about object size estimation, target imaging and signature extraction of targets [3,6,7]. The purpose of this thesis is to reduce false alarms, which are the biggest disadvantage of metal detectors, and make their use more efficient. The response of a metal detector operating in the range of 1 kHz-100 kHz to different metals has been investigated. The performance of the designed detector has been revealed by comparing the theoretical and experimental results.

In the first chapter, general usage areas of metal detectors are explained. In the second chapter, the working principle of metal detectors is explained. Detailed information has been given about pulse induction and continuous wave metal detector structures. In the third chapter, the electromagnetic model of metal detectors operating in the frequency domain is created and the answers given according to the properties of the object and according to the frequency are examined. In the fourth part, the hardware design of the metal detector

operating in 1 kHz-100 kHz frequency band is explained. The coil structure, receiver amplifier layer is described in detail.

In the last part, a remote-controllable experimental setup has been set up. Electromagnetic characteristics of objects of different sizes and features were obtained with the designed metal detector. As expected from electromagnetic analysis, distinctive signs have been obtained from objects.

2. METAL DETECTOR BASICS

In this section, basic working principle of metal detectors, general structure of metal detector technologies used, advantages and disadvantages are explained.

2.1 Magnetic Metal Detectors

They are metal detectors that can detect magnetic metal parts by taking advantage of the static magnetic field change of the earth without the need for a magnetic field source [15]. They are passive detectors since they do not have a stimulating magnetic field. Examples are magnetometers and gradiometers. Earth's magnetic field density is in the order of microtesla. Precision magnetometers and gradiometers can measure resolution with nanotes and picots. The earth's magnetic field distributions are measured with these devices and used in geophysical and archaeological studies. In addition, these detectors are used in the detection of buried ammunition without explosion.

2.2 Induction Metal Detectors

Induction metal detectors have sources of magnetic fields. The low frequency electromagnetic induction principle is based on Maxwell's equations.

$$\nabla \times \vec{E} = -\frac{\partial \vec{B}}{\partial t}$$

$$\nabla \times \vec{H} = \vec{J} - \frac{\partial \vec{D}}{\partial t}$$

$$\nabla . \vec{E} = -\frac{\rho}{\varepsilon_0}$$

$$\nabla . \vec{B} = 0$$

In the equations; $\vec{E}$ Electric field, $\vec{H}$ magnetic field, $\vec{B}$ magnetic flux density, $\vec{D}$ electrical displacement field, $\vec{J}$ free current density, ρ is the spatial charge density. When the current varying in time is applied to the transmitter coil in the metal detector heads, the $\vec{H}_{primary}(t)$ magnetic field occurs. The time-varying $\vec{H}_{primary}(t)$ magnetic field forms the electric field E on the conducting object according to Lenz's law and eddy current occurs on the conductive object. The eddy current formed creates the $\vec{H}_{secondary}(t)$ magnetic field in the opposite direction. The primary and secondary magnetic field representation is given in Figure 2.1.
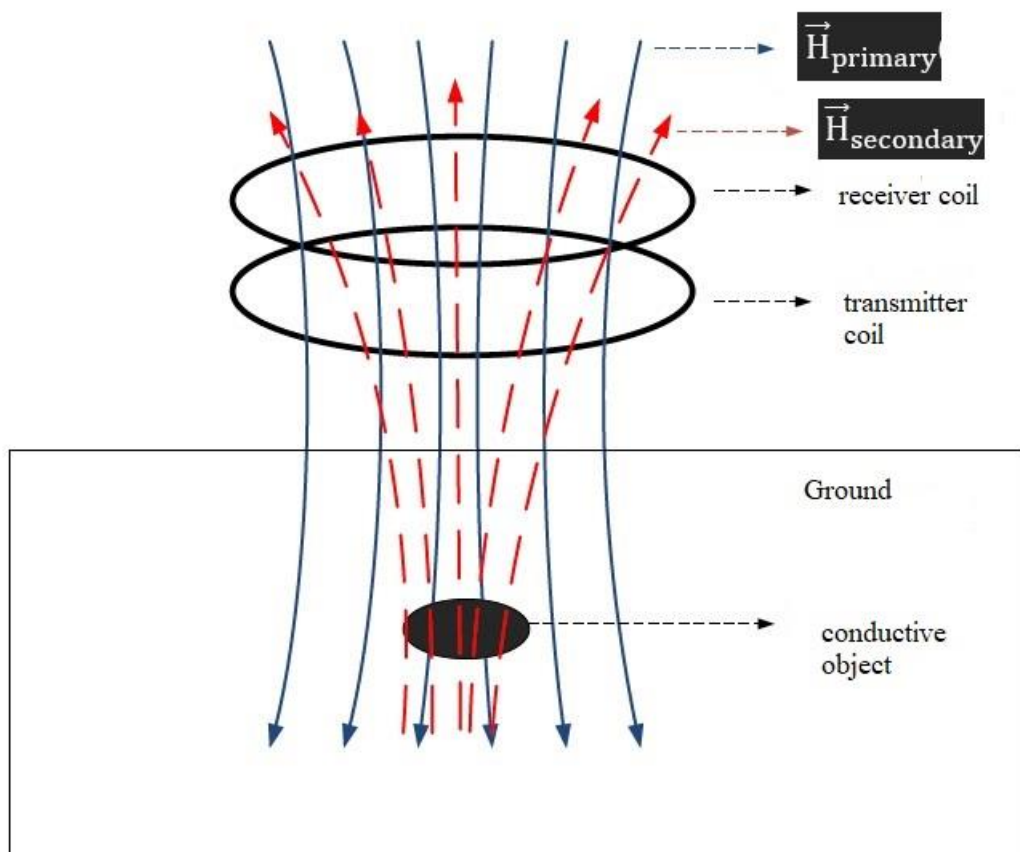
Figure 2.1: Primary and secondary magnetic field.

Voltage is induced in the receiver coil as a result of the secondary magnetic field. The $\vec{H}_{secondary}(t)$ magnetic field changes depending on the conductivity of the environment in which the target object is located and the magnetic properties and physical dimensions of the object. Eddy currents create annular currents on the surface of metallic objects. The eddy current formed depends on the conductivity constant of the conductive object. If it is high, it becomes easier to detect metallic objects. Low conductivity alloy is more difficult to detect, since low eddy currents occur in objects such as stainless steel. Magnets with low electrical conductivity cause impedance or voltage change in the receiver coil by changing the $\vec{H}$ magnetic field flux in the coil.

The electromagnetic field spreads in a conductive environment with the skin effect, decreasing by $e^{\frac{-r}{\delta}}$. r refers to the distance to the surface and the δ surface depth. The skin penetration depth f depends on the frequency f, the conductivity σ and the magnetic permeability μ of the material.

$$\delta = \sqrt{\frac{1}{\pi f \mu \sigma}} = \sqrt{\frac{2}{\omega \mu \sigma}} \cong \frac{500}{\sqrt{\sigma f}} \text{ while } \mu = \mu_0$$

Surface depths according to materials are given in Table 2.1.

Material	Conductivity σ, $(10^7 S/m)$	Magnetic Permeability μ_r	Skin Depth δ, 1 kHz	Skin Depth δ, 20 kHz	Skin Depth δ,100 kHz
Copper	5.8	1	2,06 mm	0.47 mm	0.21 mm

Alumin um	3.54	1	2.6 mm	0.5 8 mm	0.2 6 mm
Nickel	1.46	600	0.1 7 mm	0.0 38 mm	0.0 17 mm

The magnetic field created by metal detectors changes by decreasing the cube of the distance for low frequencies. The primary magnetic field on a target at a distance d from the circular coil shown in Figure 2.2 varies depending on the number of turns N, the current I, and the diameter of the coil R of the emitter coil.
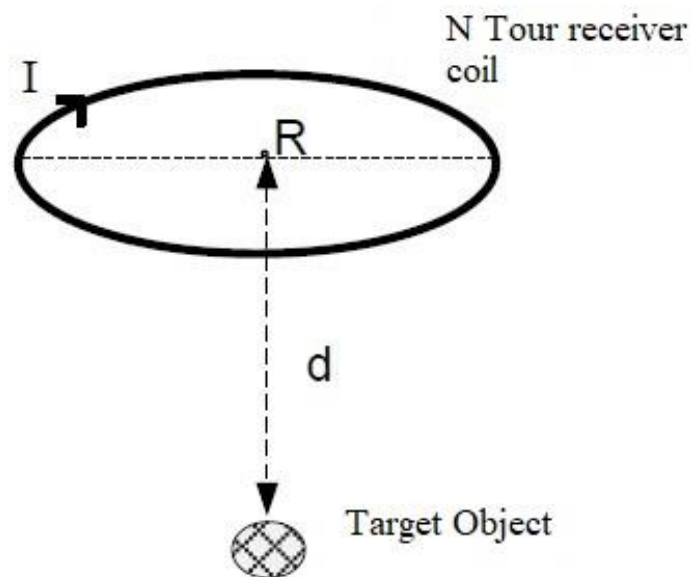
Figure 2.2: The magnetic field formed on the object.

$$B_Z(d) = \frac{NI\mu_0}{2} \frac{R^2}{\sqrt{(R^2 + d^2)^3}}$$

Accordingly, as the coil diameter is increased, deeper metallic objects can be found. However, if its diameter is too large, its sensitivity to small objects

decreases. The secondary magnetic field changes depending on the angle α between the object surface normal α and $\vec{H}_{primary}(t)$ field lines. The magnetic flux formed when the object surface is perpendicular to the magnetic field lines (α = 0°) is highest. As a result, the voltage induced in the receiver coil increases. When the magnetic field lines are parallel with the object surface (α = 90°), the magnetic flux becomes zero for two dimensional objects. As the angle α approaches 90°, the voltage induced in the receiver coil decreases. Figure 2.3 shows the conductive object at different locations.
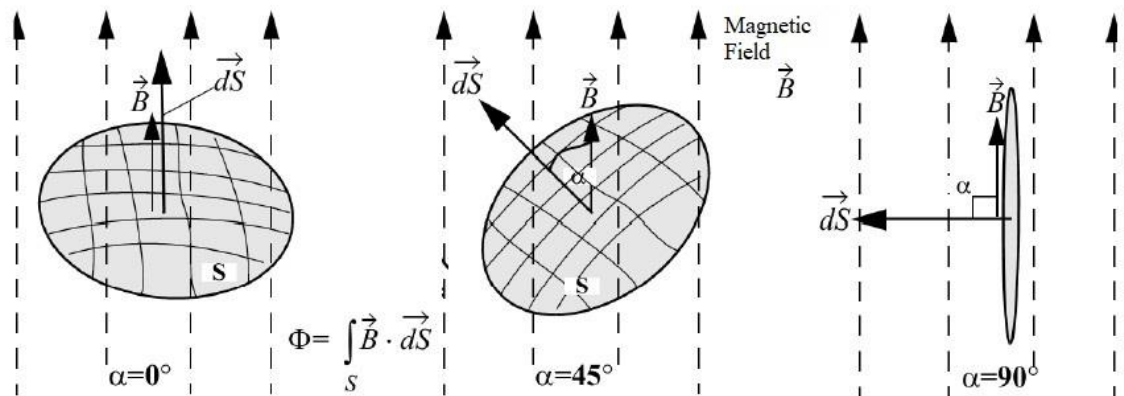
Figure 2.3 : Magnetic flux formed according to the position of the conductive target [9].

Due to the fact that the general solution in Maxwell's equations is not unique, it is impossible to obtain a definite result about the object from the signal received. In other words, the same amplitude and phase information can be taken for different objects. It is attempted to develop a solution for this with scattering theory. Ground penetrating radar (GPR) gives us information about the detection of non-metallic objects and their depth and size. This information cannot be accessed by simple signal processing. Objects are tried to be classified using complex signal processing techniques.

2.3 Coils

Coils are used to send and receive signals to the environment or to detect the magnetic field in the environment. The working logic of coils can be explained by Faraday's law. Instantaneous Vi(t) voltage occurs in the N turns wound coil.

$$V_i(t) = \frac{d\Phi(t)}{dt} = \frac{d(NA\mu_0\mu_r H(t))}{dt}$$

Magnetic flux, when $\Phi = B \times A$ is expressed

A: Coil cross section

H: Magnetic field in the coil

μ_r: Relative permeability of the coil core

The coil core may be of air or magnetic material. Its properties change according to the material in the coils. Air-core coils do not contain non-linear magnetic material. Hence the induced voltage characteristic is linear and stable. The effect of temperature on sensitivity depends on the thermal expansion of the material used. In coils this is small and negligible. Copper wire or aluminum wire can be used while producing the coil. Aluminum wire is 45% lighter. Although the conductivity of aluminum wire is lower, the coil has the same voltage sensitivity and noise.

Magnetic core coils, on the other hand, are very sensitive but less stable. Since stability and linearity are important in metal detector systems, air core coils are used [10].

2.4 Metal Detector Coil Types

The positions of the receiver and transmitter coils in metal detectors differ according to their intended use and operating technologies. There are pros and

cons compared to each other. The most commonly used coil shapes in military and hobby metal detectors are given in Figure 2.4. Single coil is widely used in pulse induction metal detectors operating with pulse signals. In continuous wave metal detectors created with a sine sign, the voltage induced to the receiver coil through the transmitter coil should be at the lowest level. Double-D, concentric coils and 4D shaped coils are used for this. They can be circular or square in shape. It does not affect performance, but in field conditions round or elliptical coils are more preferred.
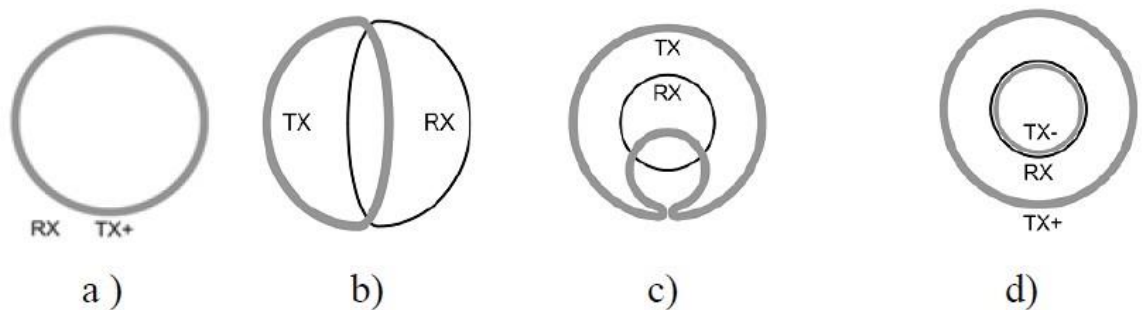
Figure 2.4: Coil types a) single coil, b) double-D coil, c) 4B coil, d) concentric coil.

The most sensitive area in single coil metal detectors are their centers. The single coil can be used as both a receiver and a transmitter. Metal can be detected by reading the secondary magnetic field with the same coil a few micro seconds after the primary magnetic field has been created. The disadvantage of this is that when factors such as environmental temperature and humidity change in the coil, the inductance and resistance of the coil may change. This also changes the characteristic. Therefore, a receiver and a transmitter coils of the same size will work more stable.

Double-D shaped coils are formed by the intersection of the receiving and transmitting coils. The distance is adjusted by making the voltage induced on

the receiver coil zero or close to zero (10 mV). The most sensitive area of the coil is the intersection of the two coils. It is widely used in treasure detectors.

Concentric coils have 2 transmit coils of different diameters. There is a 90° phase difference between the small diameter transmitter coil and the large diameter coil signals. Thus, no voltage is induced into the receiving coil from the transmitter coil. Its most sensitive area is the center of the receiver coil. It is the most commonly used coil type in treasure detectors.

2.5 Metal Detectors Working Methods

Metal detectors are divided into two according to electromagnetic field generation methods. The method that creates a magnetic field by producing a pulse is called the pulse induction method. The method that continuously creates a magnetic field with a sine sign at a certain frequency is called the continuous wave method.

2.5.1 Continuous wave metal detectors

Continuous wave metal detectors operating in frequency domain emit signals in a sinusoidal shape. According to the design purpose, the operating frequency can be in the range of 100 Hz-100 kHz. They can operate by sending signals on a single frequency or multiple frequencies in a period. Minerals in the structure of the soil behave like metallic objects. Unwanted metals such as nails and tin pieces in the soil contaminate the soil metallic. Therefore, it is difficult to find the desired metallic targets in the soil. In the continuous wave method, ferromagnetic and non-ferromagnetic objects can be distinguished. Metal detectors operating with continuous wave method are used in treasure hunting. It does not waste time by distinguishing precious metals such as silver and gold from precious metals such as nails, iron and tin.

Continuous wave detectors are also used in military mine scanning devices. An example is the Schiebel ATMID metal detector [27]. In addition, some developed detectors operate at two or more frequencies instead of a single frequency. With the data coming from each frequency used, it becomes easier to classify objects and make earth compensation. The most primitive beats operating in the frequency domain are frequency oscillator (BFO) detectors. A single coil is used as a receiver and a transmitter. The block structure is given in Figure 2.5.
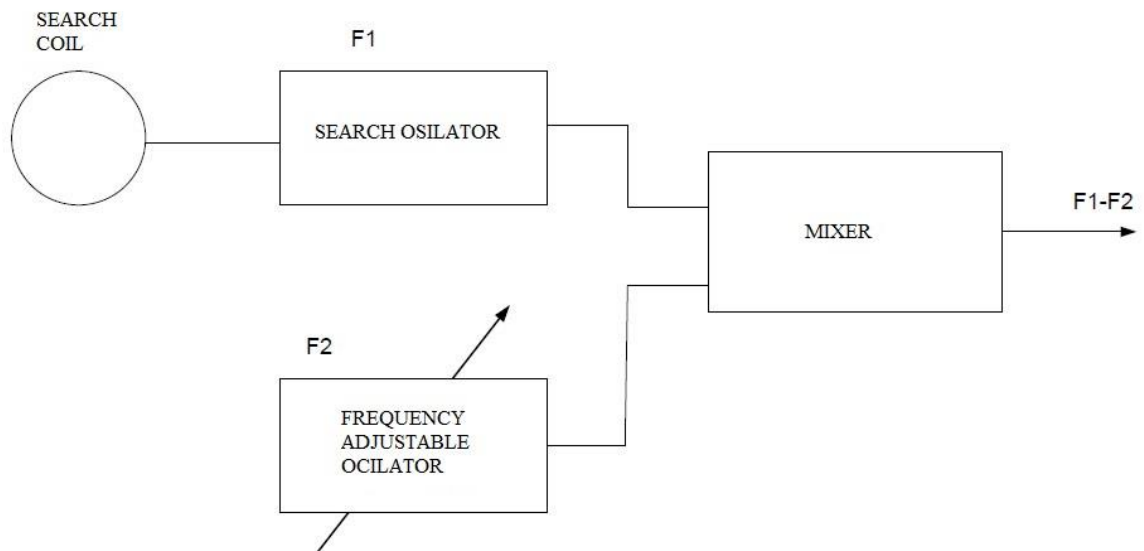
Figure 2.5 : Beat frequency oscillator.

The coil is resonated at a single frequency with a capacitance. A frequency-adjustable reference oscillator is adjusted to the desired sensitivity. Two frequencies are compared with the mixer. When there is a metallic target, the inductance value of the coil changes and consequently the resonant frequency changes. There is no signal processing at the output and the change in frequency

It is determined by giving it directly to the speaker. The shortcomings of BFO detectors are that there is no ground compensation feature. Its stability is

low in long-term operations and its performance changes by being affected by environmental factors such as temperature. The block diagram of the very low frequency detectors, which is a more complex structure, is given in Figure 2.6.
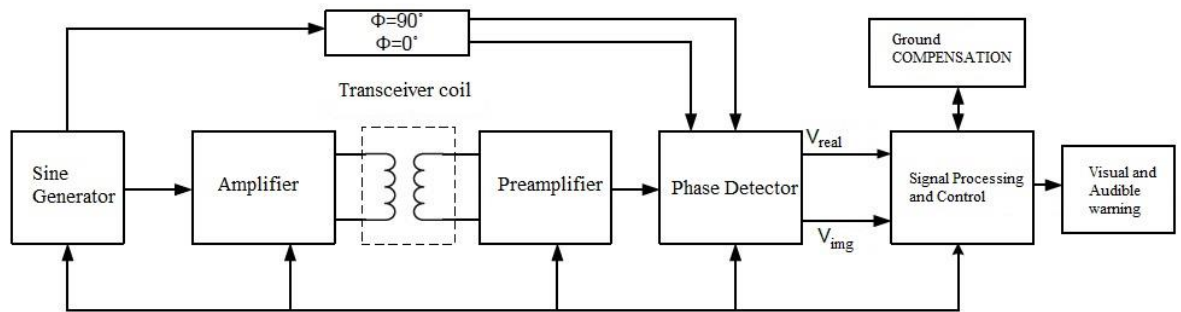
Figure 2.6 : Block diagram of continuous wave metal detectors.

A sinusoidal signal is produced with an oscillator or any signal source. With the help of amplifier, the power of the signal is increased and it radiates with the transmitter coil. The signal received by the receiving coil passes through the pre-amplifier and filter. The 90° phase-shifted state of the transmitted signal and the filtered state of the received signal enter the synchronous decoder. At its output, two values are obtained as real and imaginary. The obtained data is inserted into the signal processing procedure. In cases of metal, the detector gives an audible or visual warning according to its structure. The real and imaginary parts of the signal from the target give information about the properties of the object. It is used in the classification and detection of the object. The transmitted signal and the received signal with phase difference ϕ are shown in Figure 2.7.
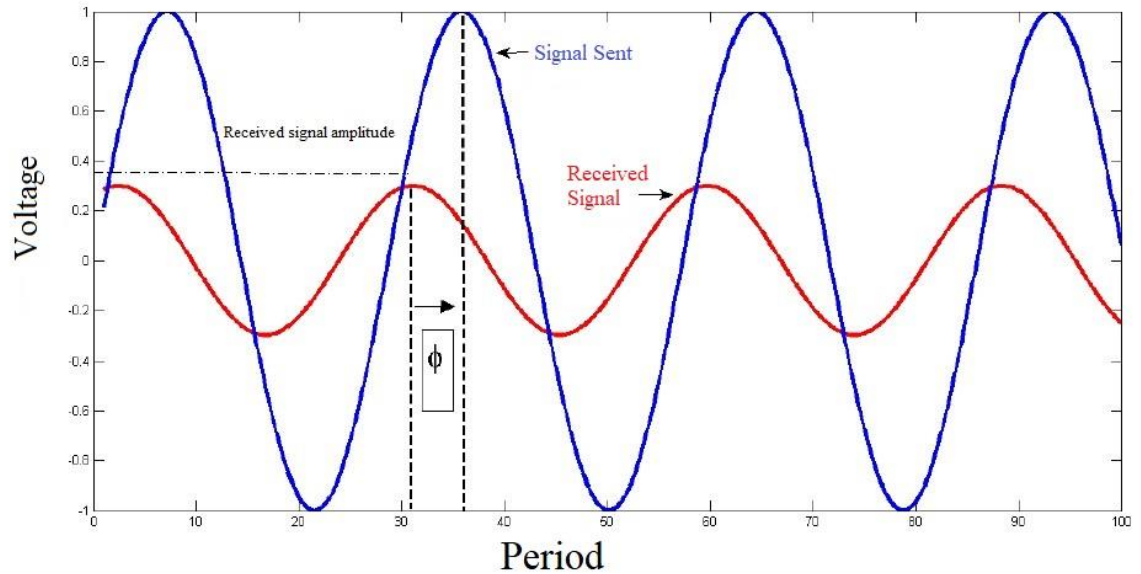
Figure 2.7 : Continuous wave metal detector sent and received signal

When we turn on the secondary voltage signal from the target:

$$V_{\text{secondary}}(t) = A_{\text{secondary}} \sin(\omega t + \varphi)$$

$$A_{\text{secondary}} \sin(\omega t + \varphi) = V_{\text{real}} \sin(\omega t) + V_{\text{imaginary}} \cos(\omega t)$$

$$V_{\text{real}} = A_{\text{secondary}} \cos(\varphi), V_{\text{imaginary}} = A_{\text{secondary}} \sin(\varphi)$$

The V_{real} component is called the coherent component. $V_{\text{imaginary}}$ component is called dichotomous component. It can be represented as $V_{\text{secondary}}(t) = V_{\text{real}} + jV_{\text{imaginary}}$ in the complex coordinate. The representation of the signal taken in the complex plane is given in Figure 2.8. Frequency selection is important in continuous wave metal detectors.
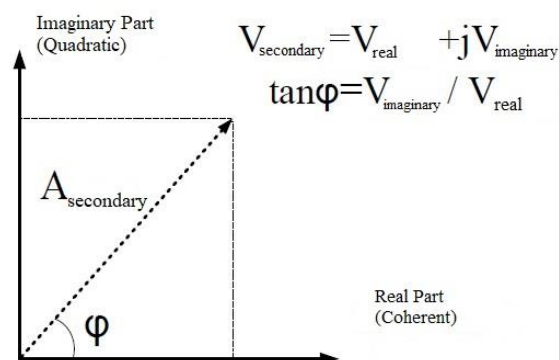
Figure 2.8: Representation of the received signal in a complex plane.

Advantages of working at low and high frequencies compared to each other and

It has disadvantages.

At low frequency:

1. Electromagnetic field penetrates deeper.

2. It is less affected by the soil structure.

3. It has low resolution compared to high frequencies.

At high frequency:

Eddy current density increases.

1. It penetrates less deeply.

2. It is more affected by the soil.

3. High resolution. So it is more sensitive in detecting small objects.

4. Since the phase angle decreases with frequency, the discrimination ability decreases.

Since two features are provided in multi-frequency metal detectors, they are much superior to single-frequency detectors. Multi-frequency metal detectors are more preferred in mine clearing and precious metal (gold, silver) searches.

2.5.2 Pulse induction metal detectors

Pulse induction metal detectors generate narrow pulses in the order of microseconds. When these high current pulses are transferred to the transmitter coil, a pulse in the order of 100 V occurs. With the instantaneous formation of a high magnetic field, an eddy current occurs on the metallic object. The secondary magnetic field is damped with time. The damping time constant can be calculated by equation (2.11).

$$\tau = \frac{L}{R}$$

The damping time depends on the coil, the conductivity, magnetic permeability and physical dimensions of the target object. Repetition frequencies can be up to 1 kHz. Higher repetition frequencies are not suitable, as it can increase the damping in the magnetic field to milliseconds. The pulse signal can be unipolar or bipolar. The double pole impact form is preferred as it does not cause any trigger on dangerous explosives. Instant narrow pulses are produced with transistors that can switch high current. After the received signal is strengthened, metallic objects are detected by reading the damping time. Block diagram is given in Figure 2.9.
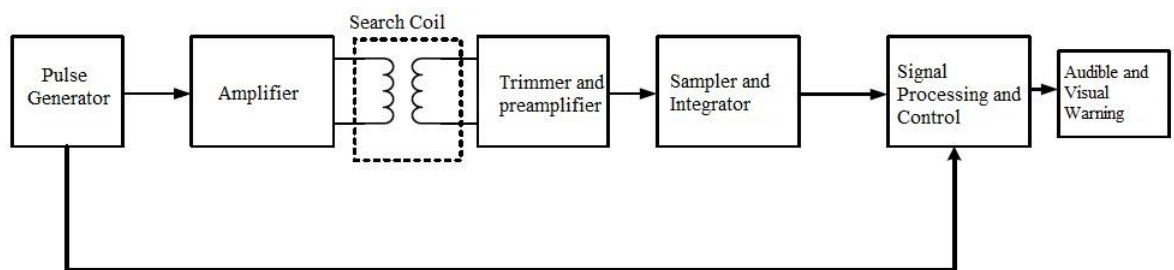
Figure 2.9 : Pulse induction metal detector block diagram.

In the sign processing part, the differences in the decay time and the damping curve are used. The damping graph for different objects is given in Figure 2.10. Very good conductive materials have lower resistance, so the damping time is longer. On the contrary, it is shorter in weak conductors.
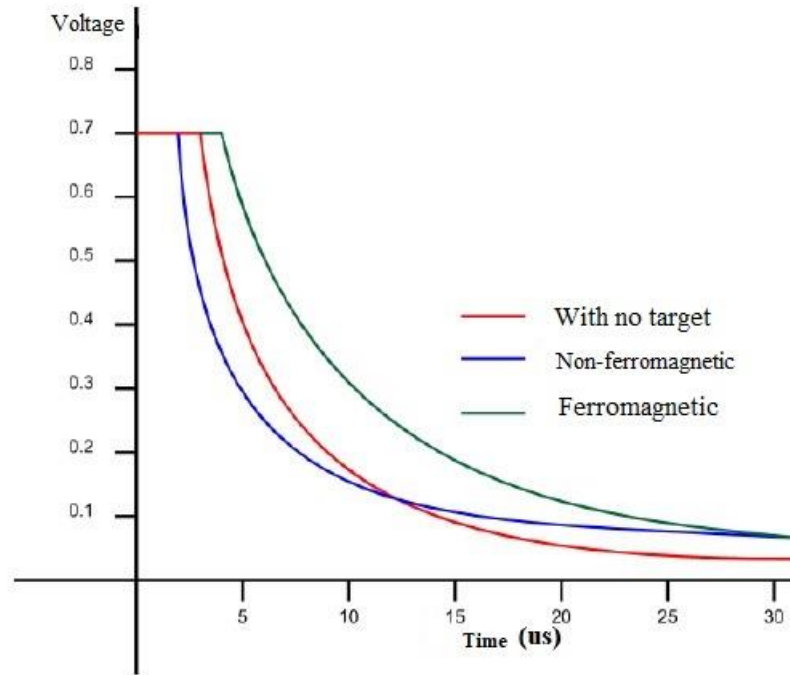
Figure 2.10 : Damping curve according to metal type [26].

Pulse induction metal detectors can penetrate deep into mineral soils and work stably. The electronic design of the detector is also simpler than metal detectors operating in the frequency domain. However, the biggest disadvantage is that it is very difficult to distinguish between ferromagnetic and non-ferromagnetic objects.

3. ELECTROMAGNETIC CIRCUIT MODEL AND ANALYSIS

Since metal detectors used in mine clearance are commercial, scientific research in this area is very limited. Especially, there are not many experimental studies on subjects such as eddy current created by objects according to their shapes (cylinder, sphere) and soil effect. Scientific studies about metal detectors working in the frequency domain generally emerge from different study areas. There are studies in the frequency space within the scope of geophysics and non-destructive testing (NdT) studies. In this section, the basic eddy current theorem and its analytical solution will be explained.

3.1 Quasi-Static Model

The Quasi static approach is used to facilitate the solution of electromagnetic problems at low frequencies. It is assumed that the distance of the target object to the transmit and receive coils and the radius of the object are smaller than the wavelength. The displacement current (J) must be negligible [16].

Let μ be the magnetic permeability constant, ε the dielectric coefficient and ω the operating frequency. In order to neglect the displacement current, the expression $\mu\varepsilon\omega^2 \ll \mu\varepsilon\omega$ must be provided. In this case it would be $\sigma \gg \varepsilon\omega$. The dependence on the insulating constant of the propagation constant disappears and the propagation constant is expressed.

$$k^2 = i\sigma\mu\omega$$

$\mu\varepsilon\omega^2 \ll \mu\varepsilon\omega$ while the expression is provided very well in metals, its value becomes $5,6x10^{-10}$ at 1 MHz in cases where conductivity is low ($\sigma = 10^5$ S/m). This situation may be valid even in soils, but this equation is not met at very low conductivity and high frequencies [9]. The conductivity of most soils is around 10^{-3}-1 S / m [13]. With this approach, the instantaneous

flux density occurring through a conductive object or medium is used when describing the magnetic field at any point in the medium. Biot-Savart law is used to calculate. When the J displacement currents are neglected, the wave equations for electric and magnetic fields are reduced and simplified [14].

3.2 Equivalent Circuit Model

Metal detectors can be modeled by creating transfer functions. The transfer function can be calculated using either the equivalent circuit model or one of the magnetic field solution methods. In both of these models, the function response F (α) is generated depending on the parameter α, also known as the induction number ø. α depends on the magnetic properties and dimensions of the object. Figure 3.1 shows the EM simple model.
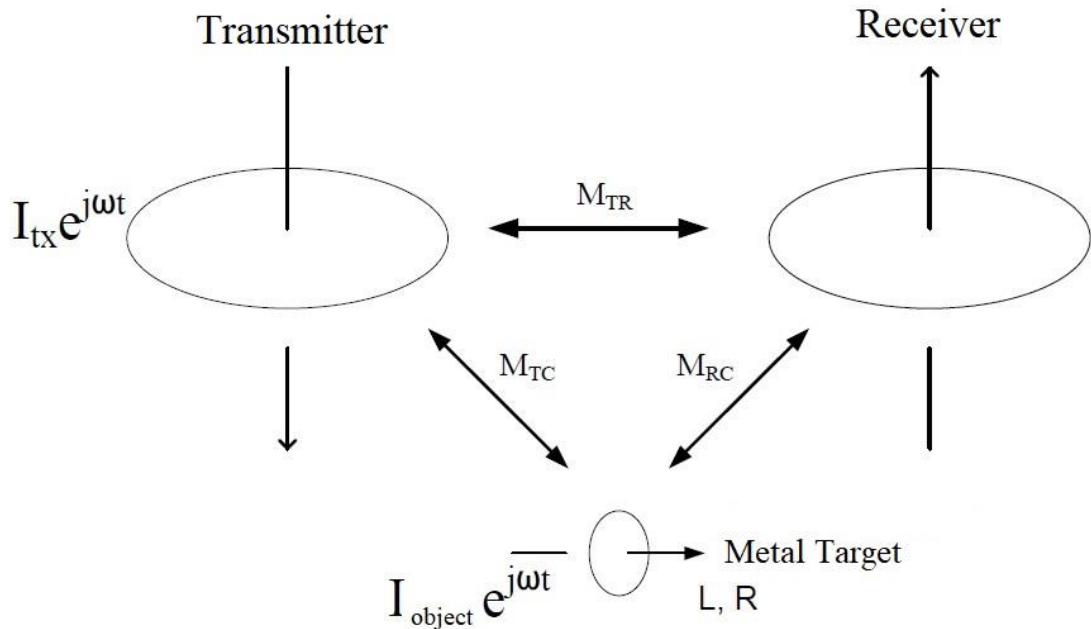
Figure 3.1 : Electromagnetic simple circuit model [9].

In order to facilitate the model and show the solution of metallic objects with finite conductivity, the target object is taken as a ring wire (a conductive

loop wire). At low frequencies, the ring wire is modeled with resistance R and series L inductance.

$$Z_{object}(j\omega) = R + j\omega L$$

According to Faraday's law, a voltage occurs on the object due to magnetic flux change in the loop wire or coil. The induced voltage is proportional to the current applied to the emitter coil. The current $I_{tx}e^{j\omega t}$ flowing on the emitter coil, $I_{object}e^{j\omega t}$ the current formed on the target object is taken.

$$V_{pbject}(j\omega) \propto j\omega I_{tx}e^{j\omega t}$$

The effect of the receiving coil, the transmitter coil and the object on each other depends on a certain value defined as mutual (common) inductance. Is the common inductance between the M_{TC} transmitter coil and the object. Current on the object

$$I_{object}e^{j\omega t} = -\frac{M_{TC}}{L}\left[\frac{j\omega L(R - j\omega L)}{R^2 + \omega^2 L^2}\right]I_{tx}e^{j\omega t}$$

The primary and secondary voltages at the receiver are expressed as in equation 3.5.

$$V_{rx-\text{primary}}(\omega) = -j\omega M_{TR}I_{tx}e^{j\omega t}$$
$$V_{rx-secondary}(\omega) = -j\omega M_{CR}I_{object}e^{j\omega t}$$

Transfer function if the ratio of voltages occurring primary and secondary in the receiver is taken as G(ω).

$$G(\omega) = \frac{V_{rx-secondary}(\omega)}{V_{rx-primary}(\omega)} = -\frac{M_{TR}M_{CR}}{M_{TR}L}\left[\frac{j\omega L(R - j\omega L)}{R^2 + \omega^2 L^2}\right] = \beta\left[\frac{\alpha^2 + j\alpha}{1 + \alpha^2}\right]$$

$$\alpha = \frac{\omega L}{R}, \beta = -\frac{M_{TR}M_{CR}}{M_{TR}L}$$

In this model, β depends on the position of the transceiver coils and their size relative to each other. If β is taken as a constant, G(ω) changes depending on the electromagnetic properties (L, R) and frequency (ω) values of the target. From here, the function response of the system can be defined as F (α) [8]. X (α) denotes the real (real), Y (α) denotes its imaginary part. The real part is

called coherent, and the imaginary part is called dichotomous. This statement applies to the equivalent circuit model of the system.

$$F(\alpha) = \left[\frac{\alpha^2 + j\alpha}{1 + \alpha^2}\right] = \frac{\alpha^2}{1 + \alpha^2} + j\frac{\alpha}{1 + \alpha^2} = X(\alpha) + jY(\alpha)$$

The above function can approximate the characteristic limits of the system. When the value approaches infinity, the X (α) term becomes 1, and the Y (α) term becomes 0. This is called the inductive limit. The function F(α) is completely real. GL (ω) = β and the response comes from the target object with the greatest amplitude. This happens when operating at high frequencies or when the conductivity is high (low resistance, R). It is observed in highly inductive targets.

When the value of α approaches zero, the X(α) term becomes 0 and the term Y(α) becomes 1. This is shown as the resistive limit. The function response becomes purely imaginary. $G_R(\omega)$ = i$\beta\alpha$. This situation is observed at low frequencies, low conductivity (high resistance, R).

In summary, at low α value initially low amplitude signals are obtained, as the α value increases, the inductive limit is approached and the amplitude increases. The phase decreases gradually to 0 ° while it is 90 ° at the resistive limit. These behavior graphs are given in Figure 3.2 [9].
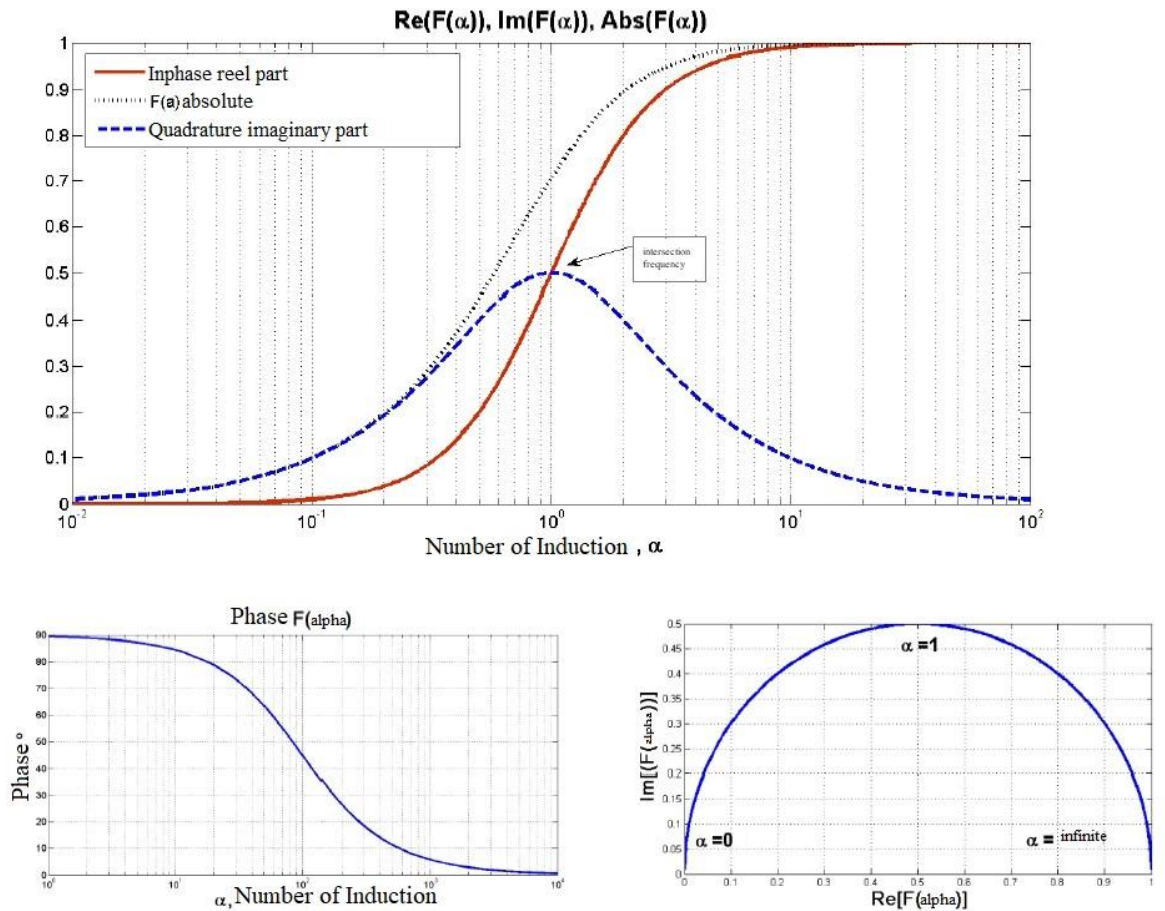
Figure 3.2 : Electromagnetic circuit model transfer function response.

The real and imaginary part of the transfer function intersect in the state α = 1.

$$f_{Intercept} = \frac{1}{2\pi\tau} = \frac{R}{2\pi L}, \tau = \frac{L}{R}$$

The intersection frequency is also expressed as equal to the resonance frequency. This feature can be looked at in the classification of objects. Because the resonance frequency changes depending on the properties of the objects [16]. The frequency at which the imaginary part peaks and the intersection frequency may not always be the same point [2]. The apex of the imaginary part depends heavily on the position and axial length of the object [17].

3.3 Constant Magnetic Field Condition

Indicates the ideal situation. Instead of a donor ring as a source, use a constant magnetic field scatterer. If the current source can only be expressed as sin (ωt), the primary magnetic flux density produced is

$$B_{\text{source}} = A_0\cos(\omega t) = \text{Re}\{A_0 e^{j\omega t}\}$$

Secondary magnetic field with ϕ phase difference

$$B_{\text{recevied}} = A_0\cos(\omega t + \phi) = \text{Re}\{A_0 e^{j\phi} e^{j\omega t}\}$$

and the phasor $A_0 e^{j\phi}$ is also expressed. Induced voltage when considered in phase space $\phi = 0$

$$V_{\text{inducted}} = -j\omega B_s = -j\omega A_0$$

and the induced current is above the conductor target impedance Z_{object}

$$I_{\text{inducted}} = \frac{V_{\text{inducted}}}{Z_{\text{object}}} = \frac{-j\omega A_0}{Z_{\text{object}}} = -j\omega \frac{A_0}{R_{\text{object}} + j\omega L_{\text{object}}}$$

If equation (3.13) is expressed as α, $\alpha = \dfrac{\omega L_{\text{object}}}{R_{\text{object}}}$

$$I_{\text{inducted}} = -j\omega \frac{A_0}{L_{\text{object}}}\left(\frac{\alpha^2 + j\alpha}{1 + \alpha^2}\right) = -j\omega \frac{A_0}{L_{\text{object}}}\left(\frac{\alpha^2}{1 + \alpha^2} + j\frac{\alpha}{1 + \alpha^2}\right)$$

$$= -j\omega \frac{A_0}{L_{object}}(\text{X}(\alpha) + j\text{Y}(\alpha))$$

With this information, three basic zone can be defined for broadband systems [2].

Resistive zone, $\alpha < 1$ and $\omega < \dfrac{R_{object}}{L_{object}}$

The imaginary part becomes more dominant than the real part. There is a 90° phase difference between the induced current and the applied field.

Intercept zone, $\alpha = 1$ and $\omega = \dfrac{R_{object}}{L_{object}}$

The real and imaginary

parts are equal to each other. There is a 45° phase difference between the induced current and the applied field.

Inductive zone, $\alpha > 1$ and $\omega > \dfrac{R_{object}}{L_{object}}$

The real part approaches the maximum, while the imaginary part approaches zero. The 180° phase difference occurs between the induced current and the field applying it.

3.4 General EM Response of Objects

F (α) in Equation 3.8 is calculated with reference to the basic circuit model. However, it is much more complex to analyze with real models of objects. The number of inductions showing the characteristic of the target object, α can be defined according to the dimensions of the object [17-19].

$$\alpha = \sigma\mu\omega l_j l_k$$

Here l_j and l_k are the linear dimensions of the target. For sphere and cylinder with radius, $\sigma\mu\omega\alpha^2$ can be taken. EM analyzes can be performed by taking $\sigma\mu\omega t\alpha$ for the disc with thickness t. Sphere shape is widely used for analytical modeling purposes. It is used because it facilitates analytical solution. Let there be two concentric coils, receiving and transmitting coils. Let the properties of the homogeneous target be defined as the radius a, the conductivity σ, and the magnetic permeability μ of the object. When the sphere-shaped target object is far enough from the coil (d >> a) or if the coil diameter is large enough (a << R) than the diameter of the object, the primary magnetic field affects the object homogeneously according to the dipole approach [17,19].

In general, the transfer function for the sphere according to the dipole approach is expressed as follows.

$$X(\alpha) + jY(\alpha) = \frac{[\mu_0(1 + k^2\alpha^2) + 2\mu]\sinh(k\alpha) - (2\mu + \mu_0)k\alpha\cosh k\alpha}{[\mu_0(1 + k^2\alpha^2) - \mu]\sinh(k\alpha) + (\mu - \mu_0)k\alpha\cosh k\alpha}$$

In the dipole approach, the transfer function is affected only by the parameters of the object. It is not affected by the position of the object relative to the coil.

3.5 EM Response of Ferromagnetic and Non-Ferromagnetic Objects

We can classify metallic objects as ferromagnetic and non-ferromagnetic materials. It significantly affects the detection of the object in electromagnetic induction sensors. Ferromagnetic materials are magnetic because they contain iron. These materials produce a strong magnetic field when a magnetic field is applied from outside. Even if the magnetic field source is removed, the magnetic moment continues in the same direction. Non-ferromagnetic materials, on the other hand, are not magnetic since they do not contain iron. Magnetic permeability constant μ_r is used to classify magnetic materials. Classification of metallic materials is given in Table 3.1.

Magnetic Moment	Diamagnetic, $\mu_r < 1$	Paramagnetic, $\mu_r > 1$	Ferromagnetic, $\mu_r \gg 1$
Type of material	Cu, Ag, Zn, Au	Al, Ti, Zr, Cr, Na	Fe, Ni, Co
Magnetization	Pretty weak	Weak	Strong

Magnetic permeability of conductive materials affects the transfer response. The graph of phase change and amplitude due to magnetic permeability is given in Figure 3.3. When the induction number α approaches infinity in non-ferromagnetic objects, the real part of the transfer function saturates and the phase angle approaches -90°. In ferromagnetic objects, the

phase approaches 90 ° when α is zero, and when the plus goes to infinity, the phase angle approaches -90 °. This is a property used to distinguish between ferromagnetic and non-ferromagnetic objects.
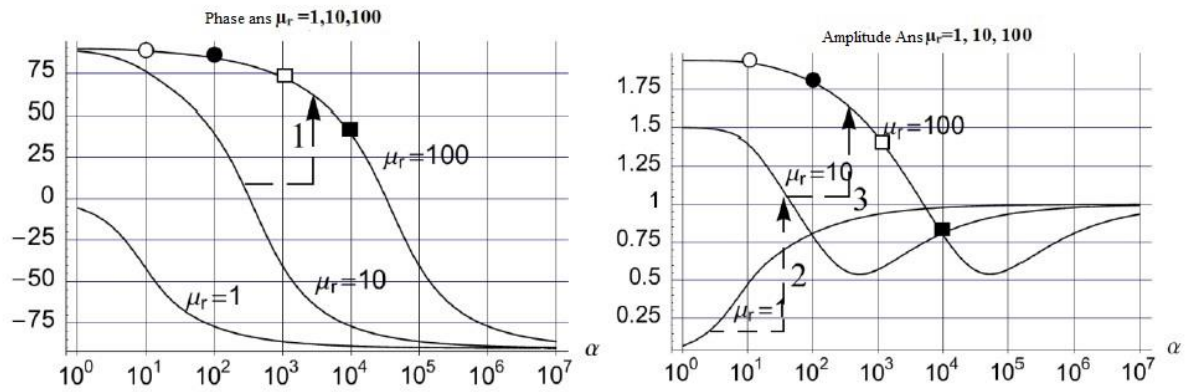
Figure 3.3 : phase response and amplitude response due to magnetic permeability [9].

While the working frequency of the object σ, a and ω is constant, the phase value increases when the magnetic permeability μ_r increases. For large α value, the phase angle becomes negative as seen in Figure 3.3. In Figure 3.4, the graph of the real and imaginary function response depending on the magnetic permeability is given. When $\mu_r = 10$, the real component decreases to negative. It is the distinguishing feature for ferromagnetic objects.
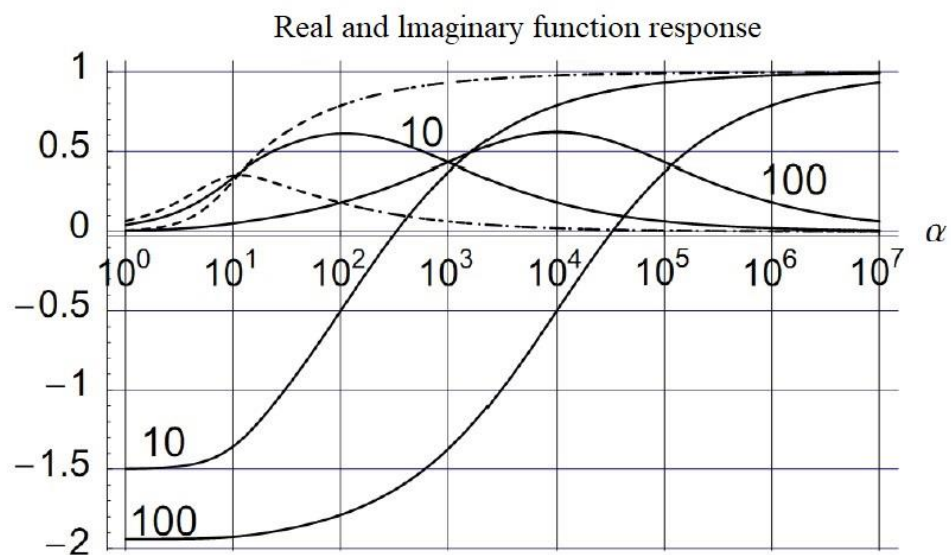
Figure 3.4 : Real and imaginary function response depending on magnetic permeability [9].

Therefore, it is not clear whether the object is ferromagnetic when operating at a single frequency. Using two or more frequencies gives more accurate results. In addition, at low frequency values, the real part of the transfer function may decrease to negative values [23].

4. MULTI-FREQUENCY HARDWARE DESIGN

In this section, metal detector design operating in 1 kHz-100 kHz frequency band will be explained. A receiver and transmitter coil is designed in accordance with the frequency range. Impedance matching and induction reset have been made in the wide frequency band. The weak signal received with the pre-amplifier design has been reinforced. The system structure is generally similar to the continuous wave metal detector structure. In continuous wave detectors operating at a single frequency, the receiving and transmitting coil operation

It is brought to resonance at its frequency. In multi-frequency studies, a linear region is used below the resonance frequency. The multi-frequency metal detector block diagram designed is given in Figure 4.1.
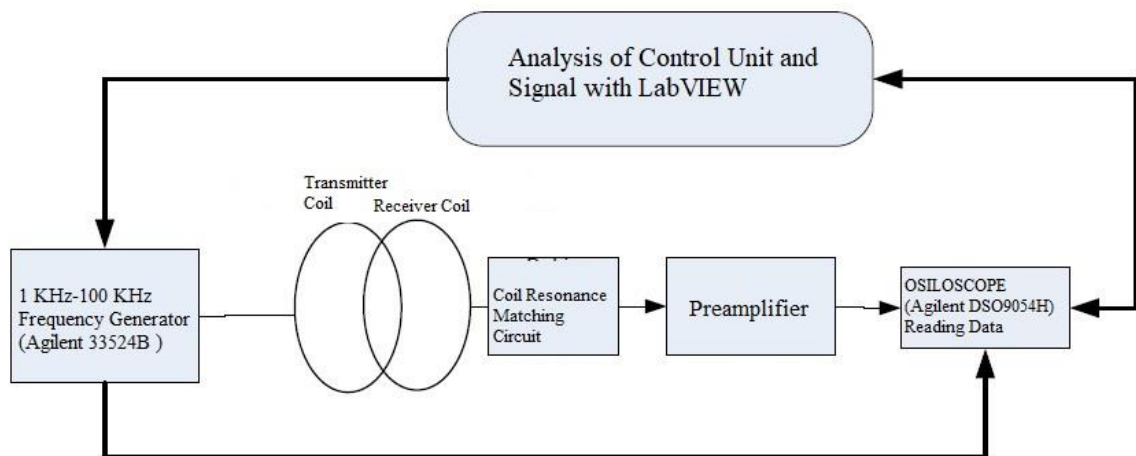
Figure 4.1: Diagram of multi-frequency metal detector.

The sine wave between 1 kHz-100 kHz was given to the transmitter coil at 1 kHz intervals. The amplitude of the sign is 20 Vpp (+10 V, -10 V). A resonant circuit was created by connecting a parallel capacity to the transmitter coil. The resonance capacity was also connected to the receiver coil. The purpose of connecting the resonance capacity is to obtain a linear operating band gap and

to make the transmission of the sent and received signal efficient by performing impedance matching. The signal received at each frequency was raised with a 33 dB amplifier. The signal sent and received with the Agilent DSO9054H oscilloscope was converted to digital data with high sampling. The phase and amplitude data of the data obtained with the LabVIEW® [28] interface program were extracted.

4.1 Design of Receiver and Transmitter Coil

Double-D coil will be used in the designed multi-frequency metal detector. The inductance value of the coils was determined according to the impedance matching. Impedance matching has been achieved by bringing the coils to resonance at the appropriate frequency.

4.1.1 Parallel resonance circuits

Resonance circuits are two-port circuits that enable the transmission of desired frequencies between the signal source and the output load. The receiving and transmitting coil must be able to transmit power at the working frequency of 1 kHz-100 kHz. The basic equivalent circuit of the coils or inductances is given in Figure 4.2.
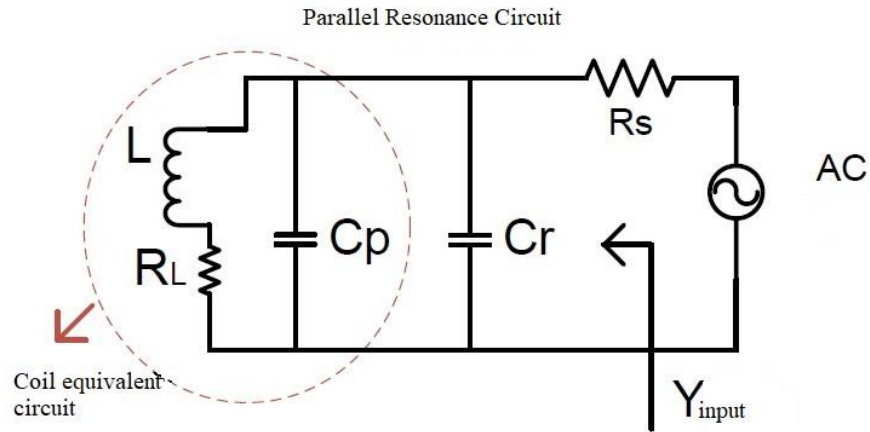
Figure 4.2 : Parallel resonance circuit and coil equivalent circuit.

The coils have L (ω) inductance and a series resistance R_{dc} series due to N turns. Parasitic Cp capacity is formed parallel to these. The Cp capacity depends on the way the coils are wound. Uneven winding and large gaps between coil wires increase the parasitic Cp capacity. This lowers the natural resonance frequency of the coil [16]. The equivalent circuit is a parallel resonant circuit. Cr >> Cp Cp was neglected in the calculations. Reactance of inductance and capacitance at a given frequency

$$X_L = j\omega L, X_C = \frac{1}{j\omega Cr}$$

It is expressed by equations. Input admittance

$$Y_{input} = j\omega Cr + \frac{1}{R_L + j\omega L} = \frac{(1 - \omega^2 LCr) + j\omega CrR_L}{R_L + j\omega L}$$

$$Y(\omega)_{input} = \frac{[(1 - \omega^2 LCr) + j\omega CrR_L](R_L - j\omega L)}{R_L^2 + \omega^2 L^2} = G(\omega) + jB(\omega)$$

$$G(\omega) + jB(\omega) = \frac{R_L}{R_L^2 + \omega^2 L^2} + j\omega \frac{(Cr^2 - L) + \omega^2 L^2 Cr}{R_L^2 + \omega^2 L^2}$$

It is found as [11]. It consists of real and imaginary parts. From here the resonant frequency of the circuit is ω_o for cases where the series resistance of the coil is neglected, where it is included ω_r:

$$\omega_0 = \sqrt{\frac{1}{LC}}, \omega_r = \sqrt{\frac{1}{LC} - \frac{r^2}{L^2}}$$

is calculated. The self oscillation frequency is smaller than the resonance frequency (o <). The two frequency inductance series resistances are equal to each other at values where R_L is small (<100k), ie the quality factor Q is too large. The impedance change depending on the frequency is given in Figure 4.3.
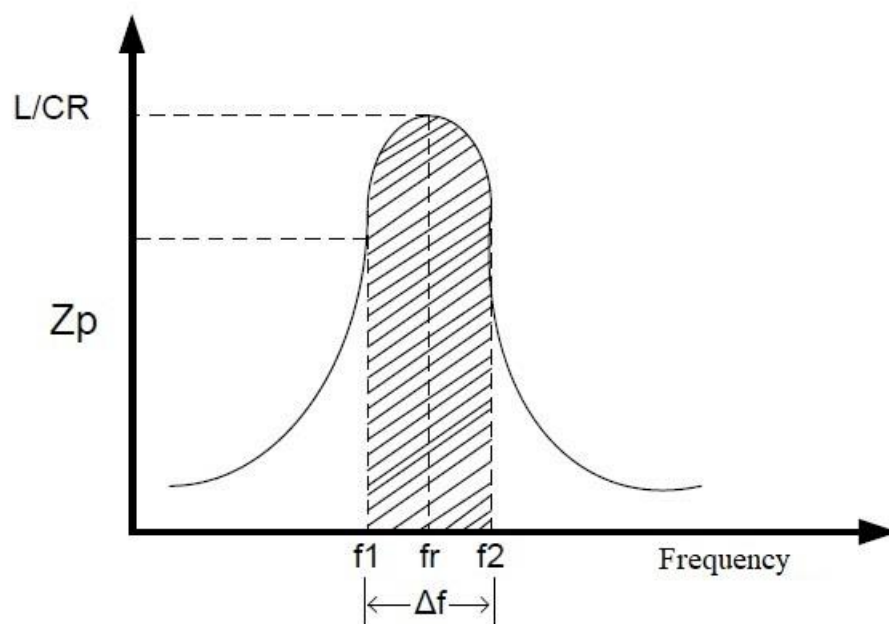
Figure 4.3: Resonance-impedance change and resonance bandwidth.

It reaches its highest value in resonance frequency. At the resonant frequency, $X_L = X_C$ and the series impedance equals the resistance R_L of the inductive element. Parallel resistance of the circuit at resonance

$$Z_p = \frac{2\pi f L}{2\pi f C x R_{dc}} = \frac{L}{C R_{dc}}$$

it is calculated by the equation. The bandwidth of the resonant circuit is the frequency range at which impedance drops by 3dB. When the quality factor of the circuit is large, the band width decreases.

$$Q = \frac{f_r}{\Delta f}, \text{ band width } \Delta f = f_2 - f_1 = \frac{f_r}{Q}$$

4.1.2 Determination of coil values

Working frequency resonance frequency is selected in single frequency metal detectors. Resonance frequency is the frequency at which the system works most sensitively and efficiently. In the multi-frequency method, the operating frequencies are within 3 dB bandwidth. The resonant frequency must be at least twice lower than the core frequency of the coil. In practical applications, it is operated with at least 5 times lower frequency [12].

The cue generator output resistance is 50 Ω. At 1 kHz the input impedance of the circuit should be at least Z_{input} 50 Ω for 3 dB bandwidth.

$$Z_{\text{input}} = R_L + j\omega L + \frac{1}{j\omega C_r}$$

Capacity shows high impedance at low frequencies. The value at which the coil is 50 Ω at 1 kHz is $j\omega L = 50 \rightarrow L = 7961 \ mH$. The graph of the voltage transferred to the coil at 2mH intervals in the range of 500 µH - 10.5mH is given in Figure 4.4.
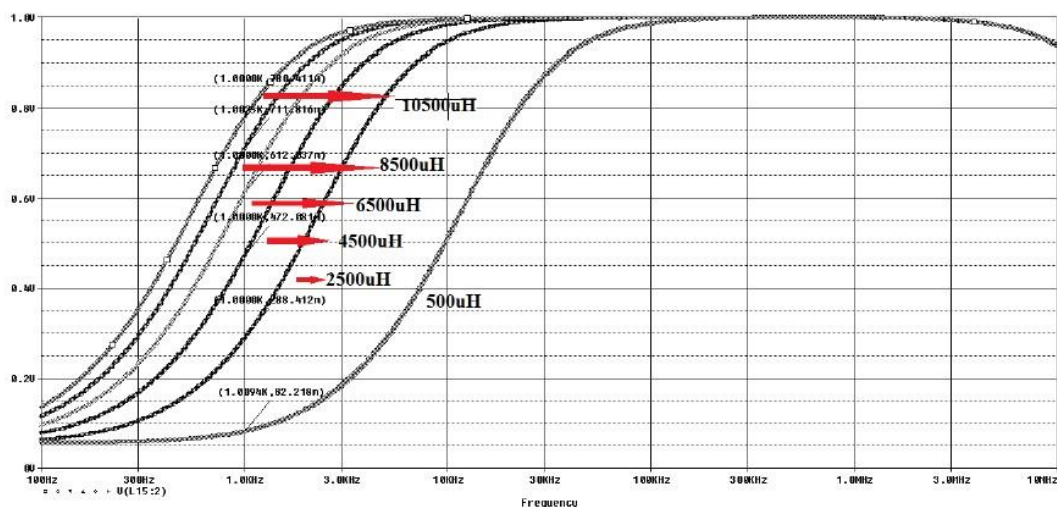
Figure 4.4 : Voltage transferred to the coil according to the inductance value.

The coil value must be greater than 8 mH. Only 8.2% of the voltage delivered at 500 µH could be transferred to the coil. Therefore, the transmitter and receiver values were taken above 8mH.

4.1.3 Preparing the coil

Receiver and transmitter coil values are calculated by equation (4.9) [20].

$$L_S = R\mu_0\mu_r N^2 \left[\ln\left(\frac{8R}{a}\right) - 2\right]$$

L_S = Calculated inductance

R = coil diameter

a = Thickness of coil wire

N = number of turns

The coil was wound so that the coil values were above 8 mH. Measured and calculated values are given in Table 4.1.

Double-D coil	Number of turns (laps)	Coil diameter	Wire diameter	Calculated inductance	Measured inductance	
Receiver coil	90	25 cm	0.35 mm	11.06 mH	9 mH	
Transmitter coil	80	25 cm	0.35 mm	8.74 mH	8 mH	

Coil measurement was made with Agilent / HP 4285A brand LCR meter. The measurement frequency was set to 75 kHz.

Transmitter and receiver resonance circuits are given in Figure 4.5. Simulations are made with the values obtained from the measurement result in Orcad Pspice program. The simulation results are given in Figure 4.6 and Figure 4.7. At 1 kHz, input impedances are higher than 50Ω as desired.
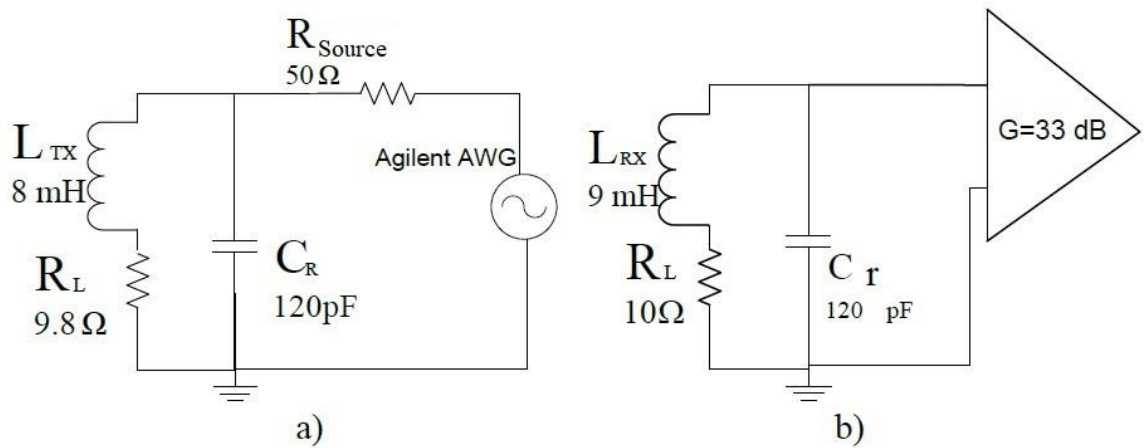
Figure 4.5 : a) transmitter and b) receiver resonance circuits.
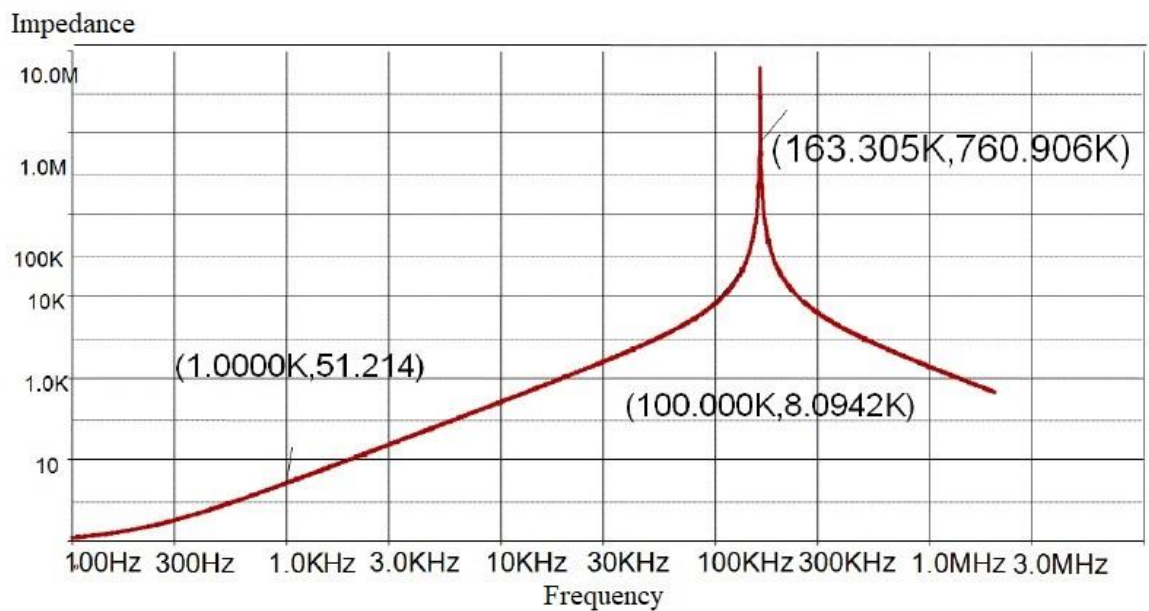
Figure 4.6 : Emitter resonance circuit simulation result.

Resonance frequencies are brought to resonance above 100 kHz. The aim is to achieve linear change in the range of 1 kHz-100 kHz.
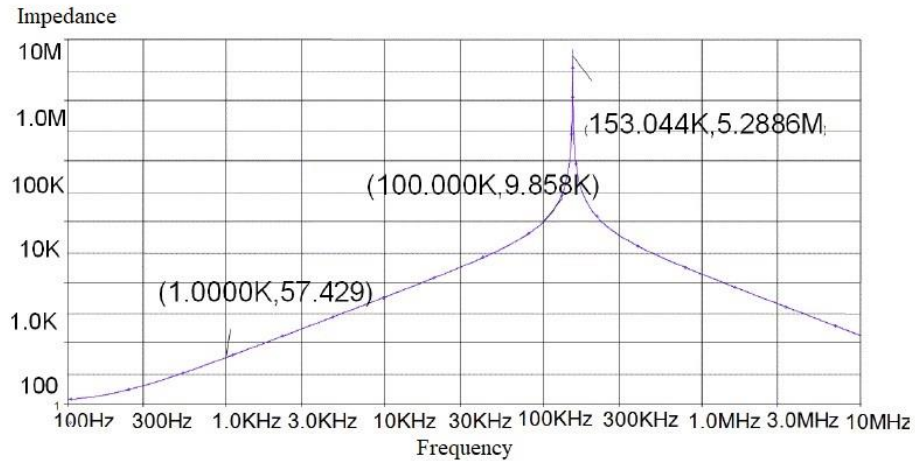
Figure 4.7 : Receiver resonance circuit simulation result.

4.1.4 Induction reset

The receiving coil (ring) position in the frequency domain is positioned in a way that minimizes the coupling effect. Otherwise, the secondary sign will disappear within the first sign. Ideally, the coupling effect is eliminated if there is an artificial, inverted phase, signal of the same amplitude at the input of the receiver.

The voltage level at the receiver is minimized when no metal is present while the two coils are induction reset. The fact that this is at a measurable level makes the real and imaginary parts of the sign readable in cases where there is no object. This works best on a single frequency. The $\vec{H}_{primary}$ and $\vec{H}_{secondary}$ magnetic field changes over a wide frequency range. Phase shift occurs in the receiver and the transmitter. The level of coupling increases at the receiver by changing the alignment [16]. In the Double-D coil, the coupling effect is eliminated by leaving a low coupling distance between the receiver and the transmitter coil as shown in Figure 4.8.
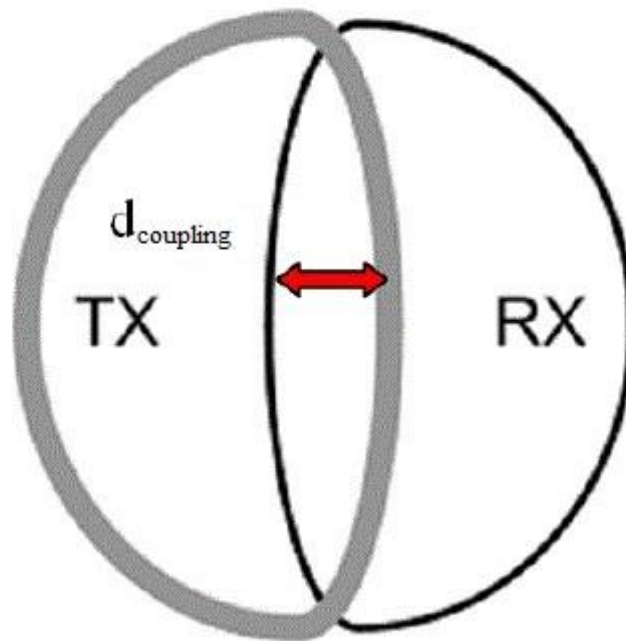
Figure 4.8 : Double-D coil and coupling distance.

4.1.5 Coil protection

The coil is covered with conductive fabric, aluminum foil or conductive paint. Magnetic field radiation is allowed only by leaving a gap in the range of 10 mm-5 mm in one place. It reduces noise by preventing external electromagnetic field interference. While the metal detector is operating, tension is generated on the outer surface of the coil. Capacitive coupling occurs between this voltage and ground. As the coil approaches or moves away from the ground will change the capacitive effect, it also changes the inductance of the coil. This causes it to be affected by the soil. The prepared double-D header is wrapped with conductive fabric. The protection fabric is connected to the ground of the circuit. It is made tight and rigid by wrapping it with polytetrafluoroethylene tape. Since the induction reset is affected by the

position of the two coils, it is enclosed in a solid plastic cap, and its shape has been preserved. The pictures of the prepared title are given in Figure 4.9.

Figure 4.9 : Open and closed version of the prepared title.

4.2 Design of Transmitter and Receiver Circuit

In single frequency studies, sine is produced by using oscillators such as Colpitts, Hartley, Armstrong. However, these oscillators cannot be used to generate signals in the broadband. The frequency of the produced signal can be changed with adjusted capacities. However, each measurement needs to be adjusted manually and it is difficult to obtain the same value in multiple measurements.

Today, digitally adjustable signal generators are available thanks to ready-made chips. When using these signal generators, attention should be paid to the ratio of total harmonic distortion (THD). When the THD ratio of the sine signal is low, a more pure sine signal is sent. This increases the sensitivity of the detector or EM sensor in the frequency domain. It allows it to penetrate deeper [12]. Direct digital signal generators (DDS) have low output power. Signal power should be increased by adding amplifiers operating in 1 kHz-100 kHz band to their output. Sound amplifiers have low total harmonic distortions up to 20 kHz. However, since the total harmonic distortions after 20 kHz are high, the sine sign is distorted.

In the thesis, Agilent 33524 series signal generator has been used as a 1 kHz-100 kHz sine source. It is preferred because the voltage level is adjustable and THD is low. It also provides convenience in the automatic measurement setup.

As a result of the secondary magnetic field, the voltage level induced in the receiver coil is low. In order for the received signal to reach a measurable level, it must be reinforced. Analog Devices AD8065 integration is used. The AD8065 operational amplifier has $7\ nV/\sqrt{Hz}$ low noise and 145 MHz wide bandwidth.

The operational amplifier should make linear amplification at the operating frequency. If the gain is kept too high, the bandwidth will be insufficient. The

open loop interference frequency of the AD8065 integrated in phase inverting structure has been given as 65 MHz. Intersection frequency in closed loop state

$$f_{-3dB} = f_{Intersection} \frac{R3}{R3 + R4} = 65MHz \times \frac{2.2k}{2.2k + 100k} = 1.4MHz$$

is found. It appears that operational amplifiers up to 1.4 MHz can be used. The impedance of the receiver coil resonance circuit varies between 57 Ω-9.8 kΩ in the range of 1 kHz-100 kHz. In order to have impedance matching with the amplifier, the input impedance of the amplifier was determined as R4 / R3 = 1.8 kΩ. R2 = 2.2 kΩ. Undesired signs are suppressed with low-pass and high-pass filters in the circuit. A high pass filter is designed with C3 and R6. Low frequency signals such as power line noise and motor noise are attenuated by a high pass filter.

$$f_{high\ pass} = \frac{1}{2\pi C_3 R_6} = 72Hz$$

With the low-pass filter, high-frequency components formed in power supplies and unwanted signals in the environment are suppressed.

$$f_{low\ pass} = \frac{1}{2\pi C_1 R_4} = 723.4kHz$$

The receiver amplifier circuit is given in Figure 4.10.
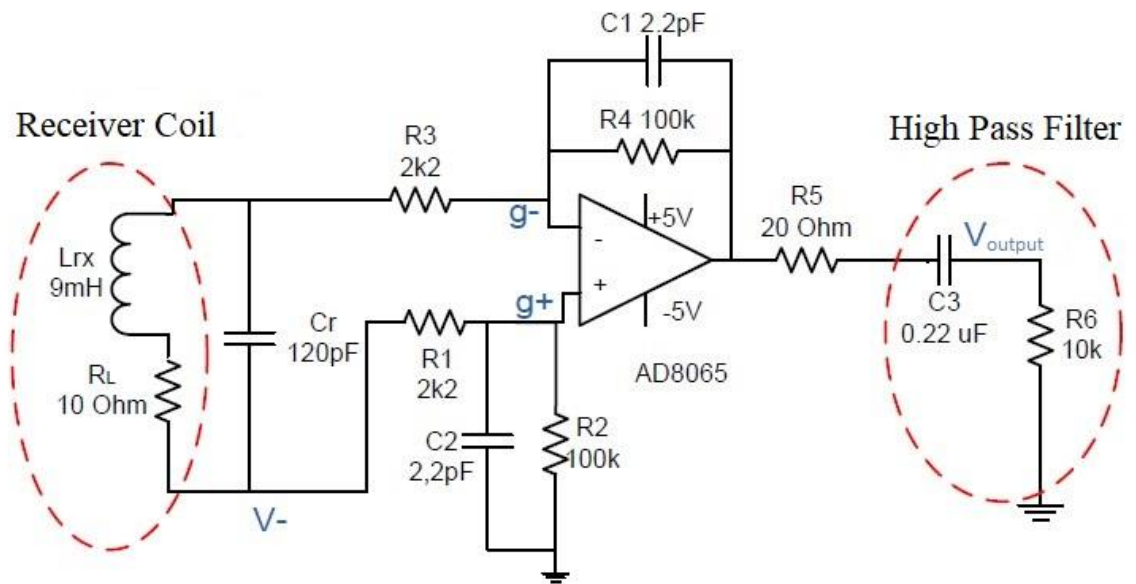
Figure 4.10 : Receiver amplifier circuit.

Output voltage of the circuit:

$$g+= \frac{R2}{R2 + R1}V_-$$

$$V_{\text{output}} = g_- + iR4 = g_- + \left(\frac{g_- - V_+}{R3}\right)R4 = -\frac{R4}{R3}V_+ + \frac{1 + \dfrac{R4}{R3}}{1 + \dfrac{R1}{R2}}V_-$$

$$= -V_+\left(\frac{R4}{R3}\right) + V_-\left(\frac{R2}{R2 + R1}\right)\left(\frac{R3 + R4}{R3}\right)$$

The equation becomes simpler if R1 = R3 and R4 = R2. Common-mode gain decreases and CMRR rate increases, suppressing unwanted signals.

$$V_{\text{output}} = -\frac{R4}{R3}(V_+ - V_-) = -\frac{100k}{2k2} = 45,45 \cong 33.1\text{dB}$$

Parasitic capacities at the output can cause unwanted oscillation and peak amplitude. R5 resistor in series is put on the output to prevent it. It provides isolation of output and capacitive load. 20 Ω is the value recommended by the integrated manufacturer.

The 4 cm x 4 cm sized receiver and transmitter circuit was drawn with the Altium program. The PCB of the board is given in Figure 4.11. The post-string voltages and gain value of the prepared card were checked. After making sure that it works correctly, tests were started.
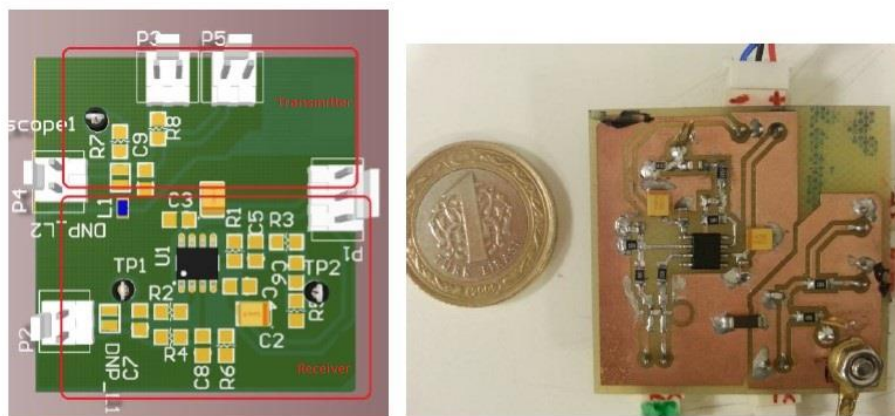
Figure 4.11 : Prepared receiver and transmitter card.

5. METAL DETECTOR DATA ANALYSIS

Data were taken from the test objects under laboratory conditions with the prepared metal detector. Electromagnetic theoretical responses of objects in frequency domain are compared with experimental results.

In the thesis, data were collected in the range of 1 kHz-100 kHz, with 100 different frequencies at 1 kHz intervals. Agilent 33521B AWG was used as the cue generator. Since the oscilloscope is more reliable in converting data to digital, analog-digital converters were not used at this stage. Agilent DSO9054H oscilloscope was used. The signal generator and oscilloscope were controlled by the LabVIEW® program. LabVIEW® program is a software platform developed by National Instrument. Thanks to its visual programming language, it provides an effective and easy solution for controlling measuring devices. The required phase and amplitude data were obtained by processing the received data with the LabVIEW® program.

5.1 Establishment of Experiment Setup

Prepared experimental setup is given in Figure 5.1. The search coil with coils is placed on a metal-free box. The designed electronic card has receiver and transmitter circuits. With the signal sent, test points have been placed at the output of the amplifier. The marks were measured by connecting the measuring tips of the oscilloscope to these points. The measuring setup is installed away from metallic objects. It is prevented from being affected by noise by keeping it away from switched power sources emitting low frequency noise and light sources such as fluorescent.
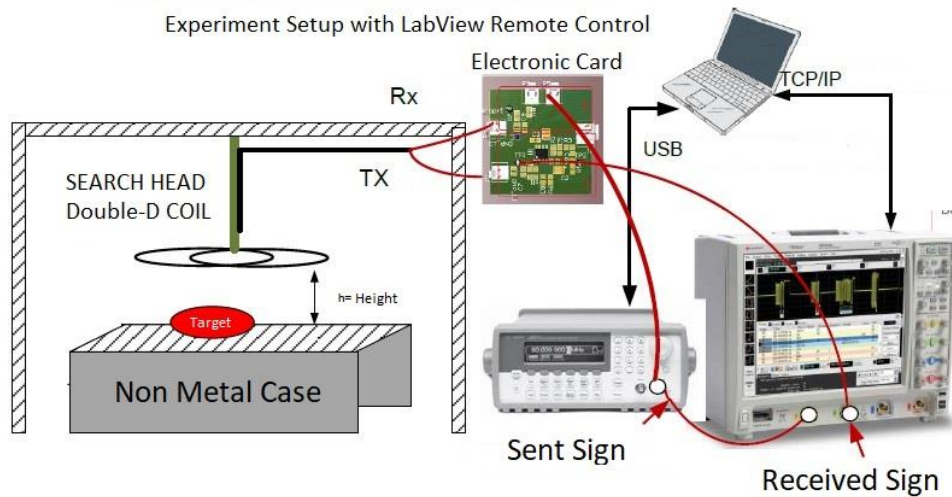
Figure 5.1 : Multi-frequency metal detector test setup.

The LabVIEW® program ensures that the data is taken in the same way every time, without touching the experimental setup. The test environment is given in Figure 5.2.
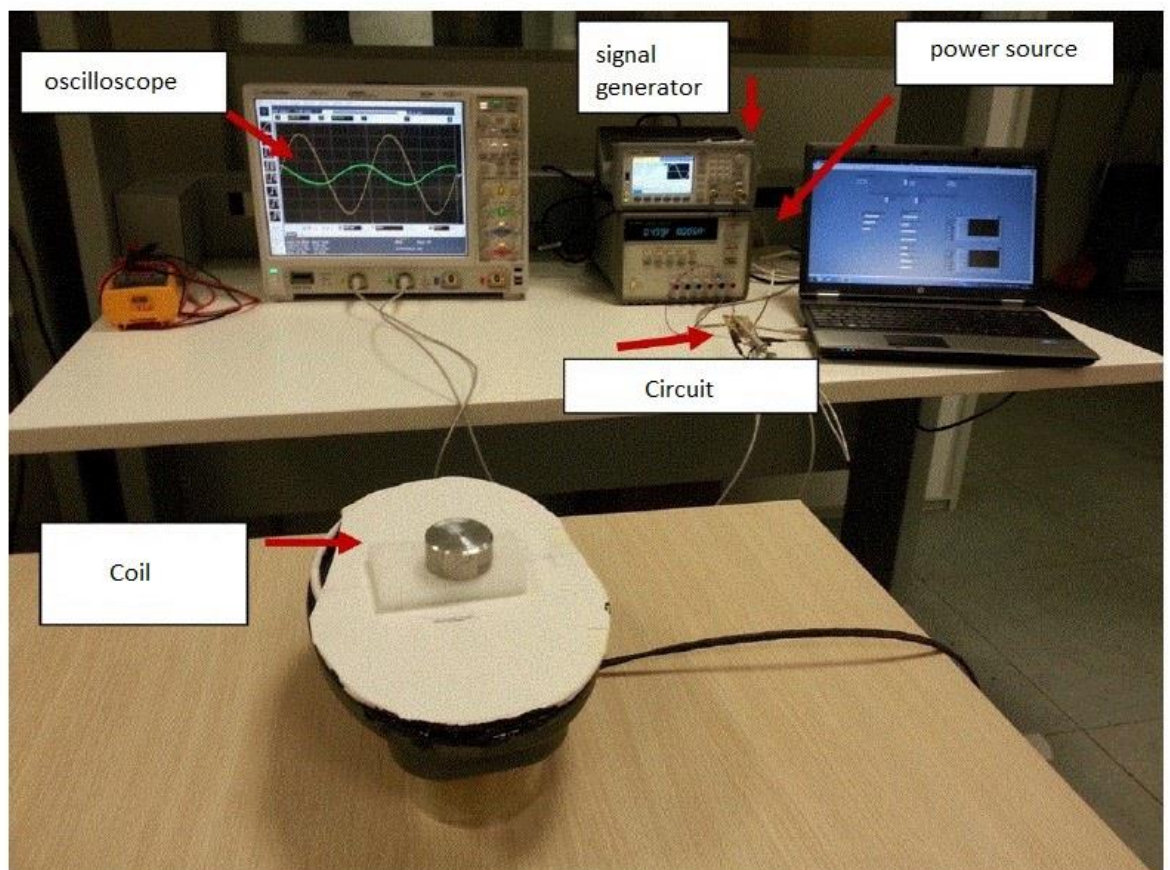
Figure 5.2: Test environment.

5.2 Remote Control Program Interface

The settings of the signal generator and oscilloscope are made in the program interface. In the program, each frequency measurement is repeated 5 times. The data taken were recorded in two different files as phase and amplitude. Flow diagram of the program is given in Figure 5.3.
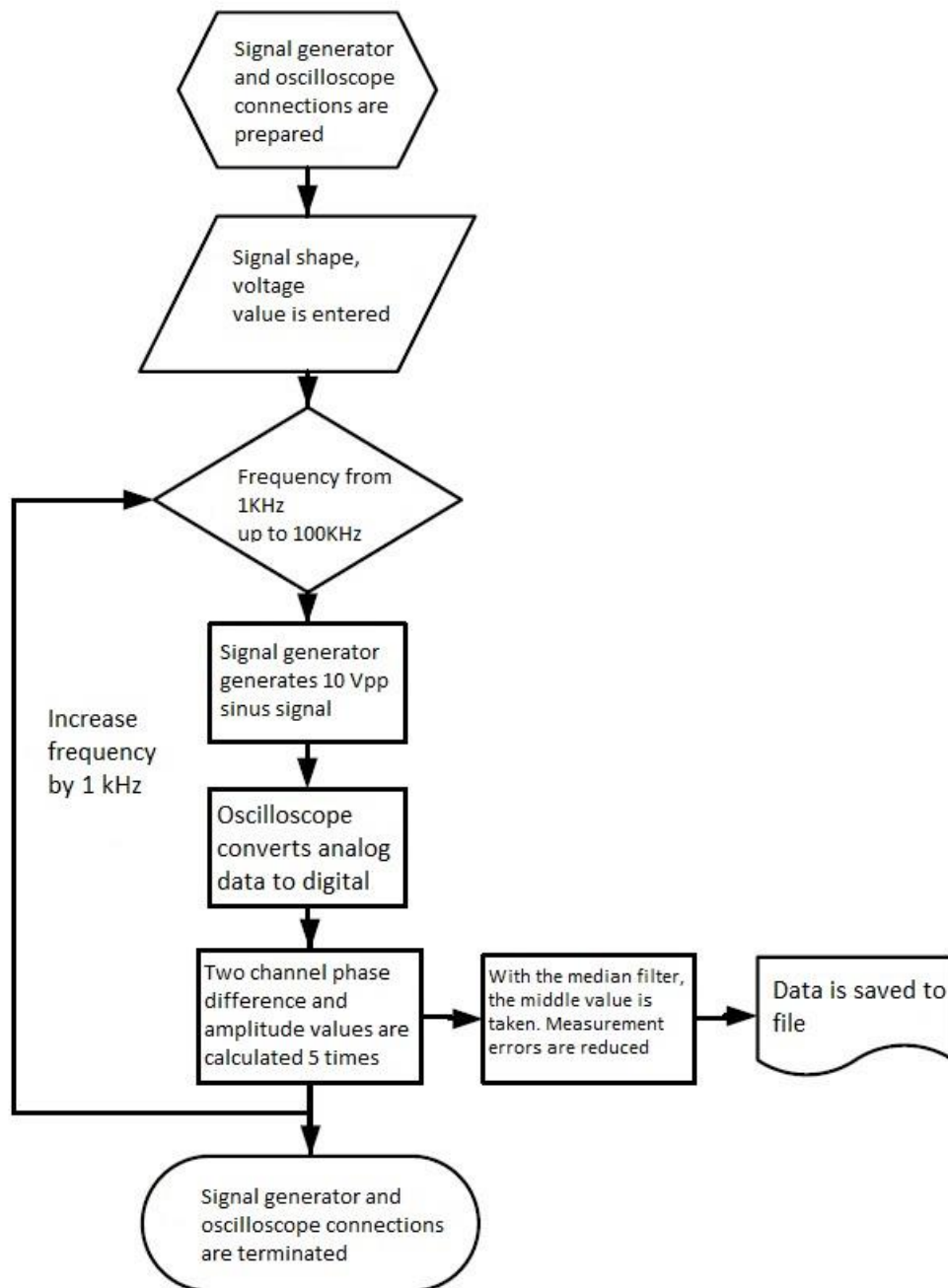
Figure 5.3 : Data collection flow chart.

The enhanced signal graphics coming from the sent sign and object are drawn in the interface. The phase information of both signs is designed to be followed in degrees from the interface. Only the phase information of the received signal may not be meaningful data. Phase information shifts according to the point where the oscilloscope captures the signal. Therefore, stable phase information is obtained by taking the phase difference of the two channels. The amplitude ratio expresses the ratio of the signal at the receiver output to the transmitter signal. The appearance of the LabVIEW® interface is given in Figure 5.4.
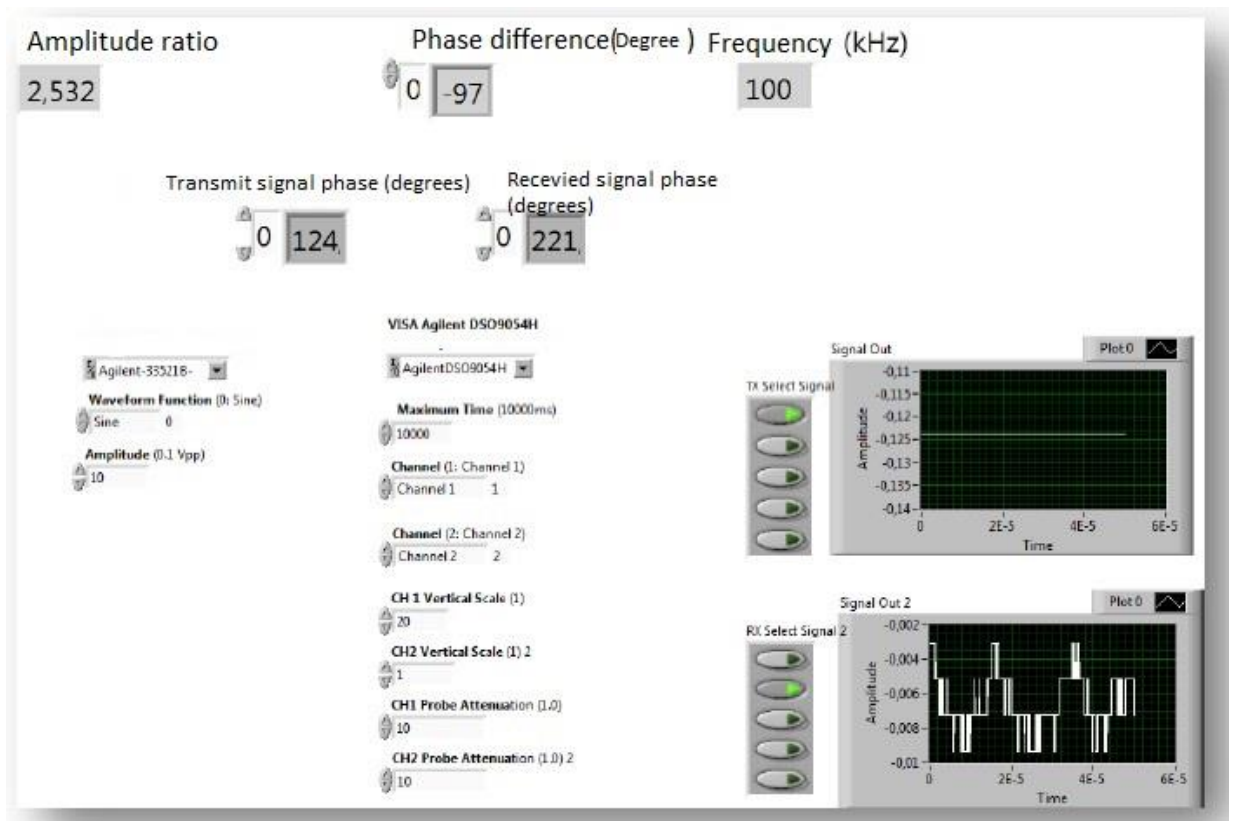
Figure 5.4 : LabVIEW® control interface.

5.3 Adjusting the Signal Generator and Oscilloscope Settings with LabVIEW®

The Agilent 33521B signal generator is connected to the computer via USB. With the adjustment boxes provided by the program, the signal generator control scheme has been created. The shape and amplitude of the sign has been made adjustable by the user. The block diagram is given in Figure 5.5.
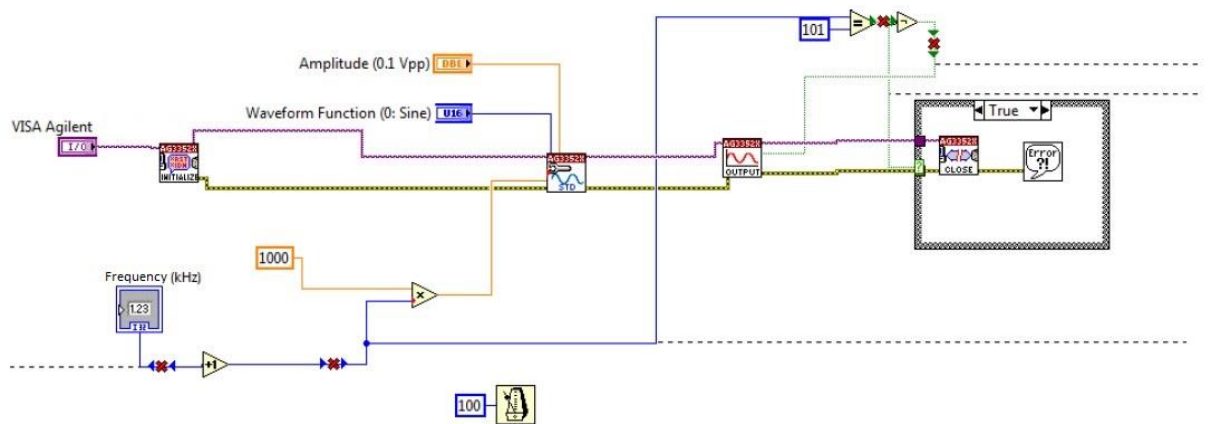
Figure 5.5 : Signal generator control block diagram.

When the program is run, a 1 kHz 10 Vpp sine wave is generated. The transmitted signal is increased by 1 kHz at each stage and continues up to 100 kHz. After the frequency is set, the oscilloscope transfers the digital data in its memory to the LabVIEW® process blocks at the rate of time division. The phase and amplitude values of the signs are calculated with the data obtained. This process is repeated 5 times after waiting 50 ms. At the end of 100 kHz, the computer-device connection is terminated.

The Agilent DSO9054H sets the time scale and voltage scale by automatic adjustment when the oscilloscope is first started. It automatically adjusts at 1 kHz, 7 kHz, 20 kHz, 40 kHz and 70 kHz in order to accurately measure the

incoming signal. Converts the signals attached to the measuring tip to digital data with channels a and b. The block diagram is given in Figure 5.6.
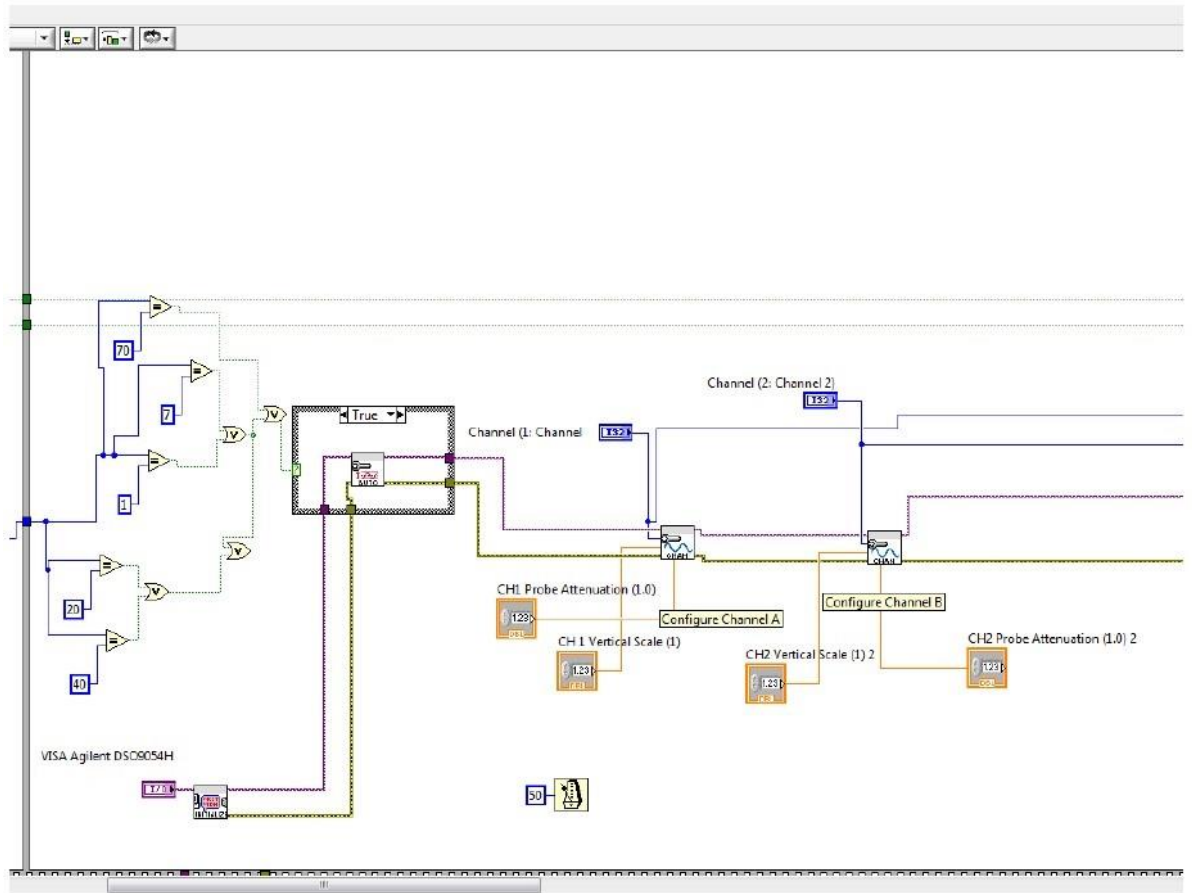
Figure 5.6 : Oscilloscope control block diagram.

5.4 Data Processing with LabVIEW®

The data from the oscilloscope was made by using LabVIEW® process blocks. Amplitude and phase data are calculated by fast Fourier transform (FFT) to examine the data from test objects in frequency domain. As a result of FFT, quadrature and in-phase data are obtained. Conversion is made using these values for phase and amplitude data. The block used in the LabVIEW® program gives the value of phase and amplitude. Quadrature and in-phase data were obtained by inversion. The block diagram created in Figure 5.7 is given.

The measurements were repeated 5 times at each frequency and the obtained values were recorded.
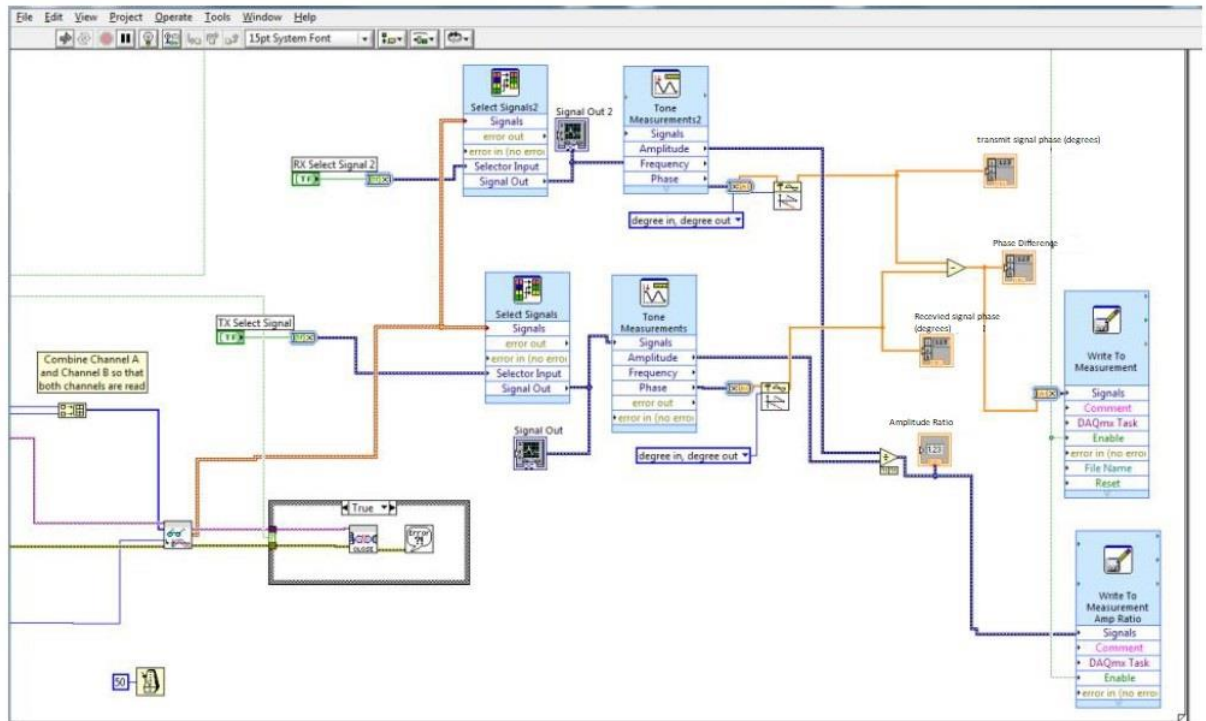
Figure 5.7 : Processing and recording block diagram of LabVIEW® Oscilloscope data.

5.5 Test Objects

7 different objects were used to test the designed multi-frequency metal detector. The test items are given in Figure 5.8.

The ferromagnetic iron cylinder is R = 8 cm in diameter and h = 2 cm high. The dimensions of non-ferromagnetic aluminum cylinders are R = 4 cm and h = 3.4 cm, with a diameter of R = 4.5 cm and a height of h = 2.2 cm, respectively.

PMN and TS-50 anti-personnel mines were used to see the characteristics of the mines. They are difficult to detect because of their low metal density. The mines used are not real and have the same metal density and physical structure. 50 Cent and iron bars were used to see the effect of metallic objects

found in nature, mixed with mines. The iron bar is R = 1cm in diameter and h = 5.5cm in height.
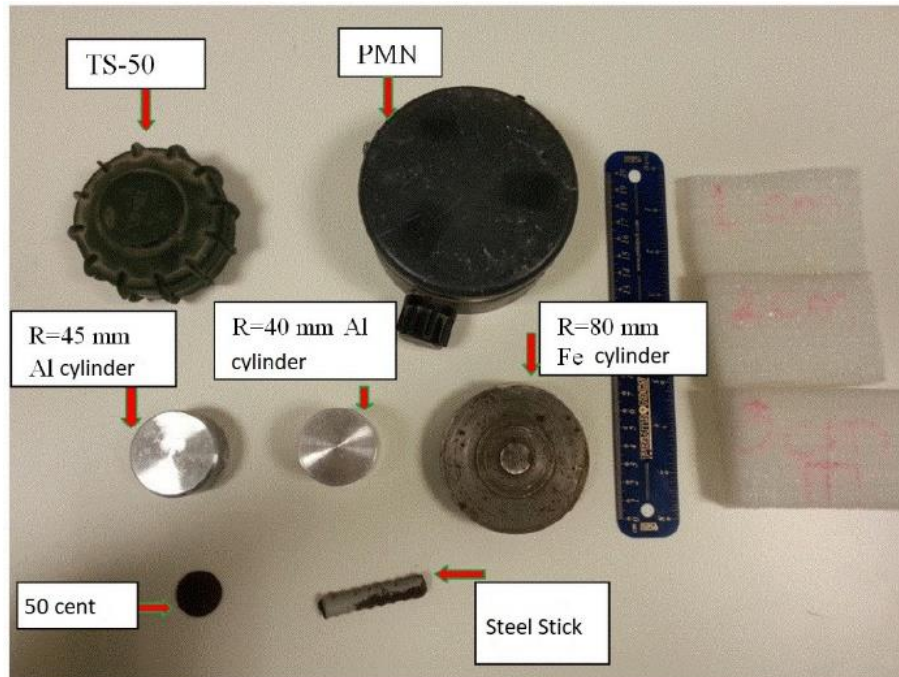
Figure 5.8: Test objects.

5.6 Processing of Received Data

The data obtained were analyzed using the MATLAB® program. The evaluation was made by looking at the real and imaginary parts of the signs as well as the phase and amplitude data. The phase and amplitude data of the signals taken with the LabVIEW® program are extracted. The phase and amplitude values are calculated by taking the FFT of the signs. Since the capturing point of the signal of the oscilloscope can change in the phase angle values of the marks, there may be 360 shifts. For example, the phase measurement that goes around 160˚ also comes as -200˚. The corrected version is given in Figure 5.9.
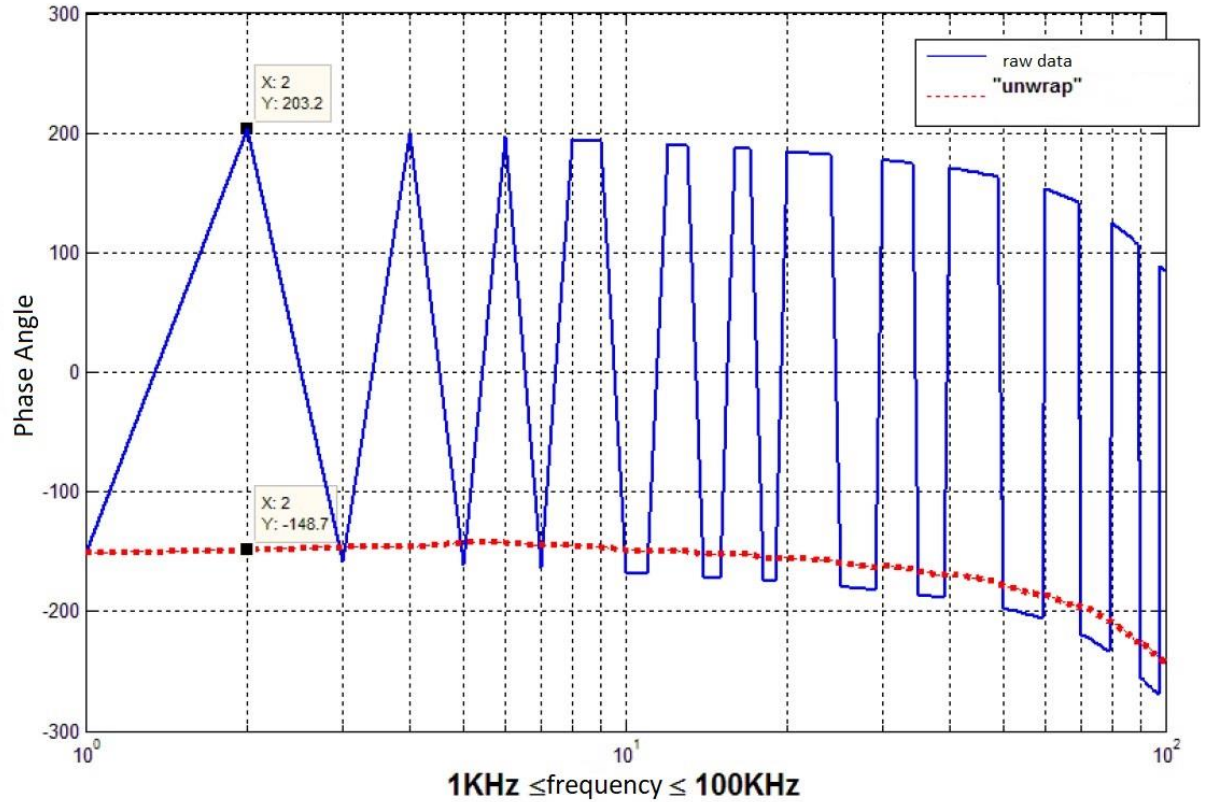
Figure 5.9: Phase verification.

5.7 Evaluation of Results

For 7 different test objects, data were collected for different distances of 10 mm, 20 mm and 30 mm from the metal detector. The phase and amplitude changes of the objects depending on the distance and the change of the coherent-quadrature values in the frequency range have been investigated. The values obtained from the 1 kHz-100 kHz multi-frequency metal detector will be compared with the EM analytical solution results.

5.7.1 Results of 4 cm diameter cylindrical aluminum

Phase and amplitude measurement results are given in Figure 5.10. The primary magnetic field increases exponentially as metallic objects get closer

to the metal detectors. When the amplitude ratio graph is examined, the change between 10 mm-20 mm and 20 mm-30 mm changes exponentially.
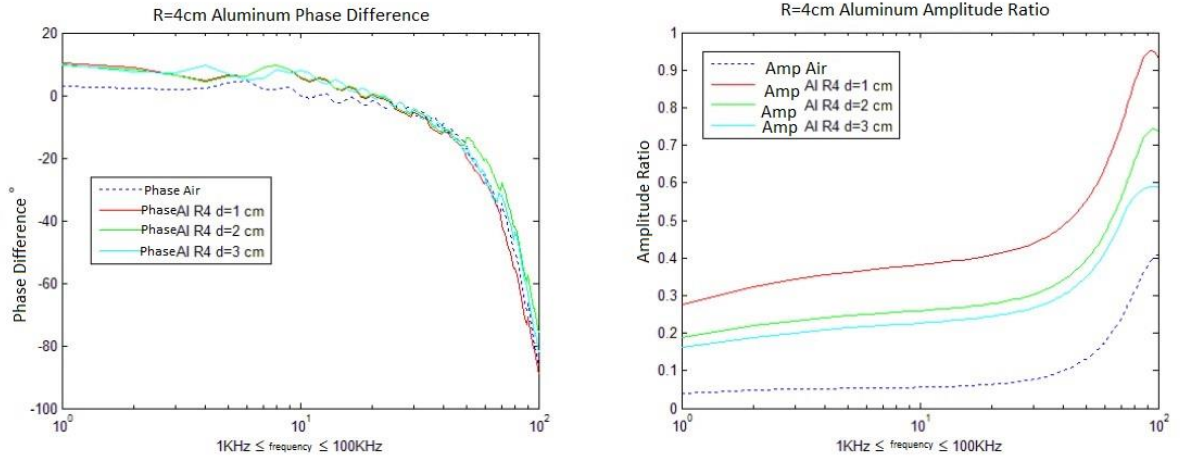
Figure 5.10 : R=4 cm Aluminum Cylinder phase diff and amplitude ratio.

Aluminum is a non-ferromagnetic metal. The phase angle in the measurement results is 10 ° at 1 kHz. As the frequency increases, it gradually decreases. It reaches -90 ° at 100 kHz. Theoretically it is expected to range from 0 ° to -90 °. It was observed that the measurement result and the theoretical result were compatible with each other.

It is seen that the phase angle in aluminum object does not depend on the height. The measured quadrature and coherent data are given in Figure 5.11.
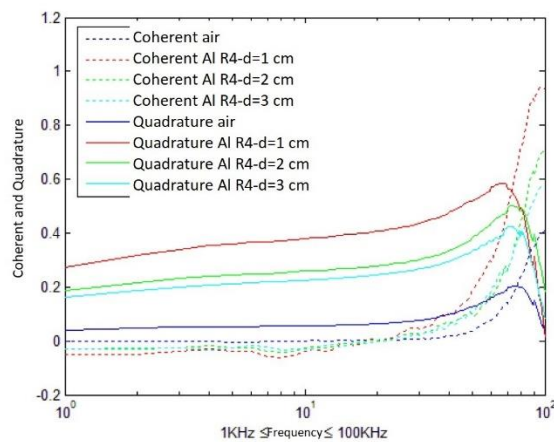
Figure 5.11 : Measurement of R=4 cm aluminum cylinder quadrature and coherent.

The results coincide with the theoretical values. Coherent (real) values vary depending on the distance of the object. The absence of any metal is shown as weather data. As the object approaches the coil, the intersection frequency decreases with its idle coherent value. It was measured as 18 kHz for d = 10 mm, 22 kHz for d = 20 mm, and 23 kHz for d = 30 mm. After the intercept frequency, the coherent curves rise above the air curve.

5.7.2 Results of 4.5 cm diameter cylindrical aluminum

R = 4.5 cm diameter aluminum cylinder measurement result is given in Figure 5.12 and Figure 5.13. The diameter and surface area are different from the R = 4 cm diameter aluminum cylinder. The voltage induced in the receiver coil is expected to increase as the surface area perpendicular to the $\vec{H}_{primary}(t)$ magnetic field increases. When we compare the amplitude ratio data, the voltage generated by an aluminum cylinder with a diameter of R = 4.5 cm is higher. Phase does not depend on the height in either object.
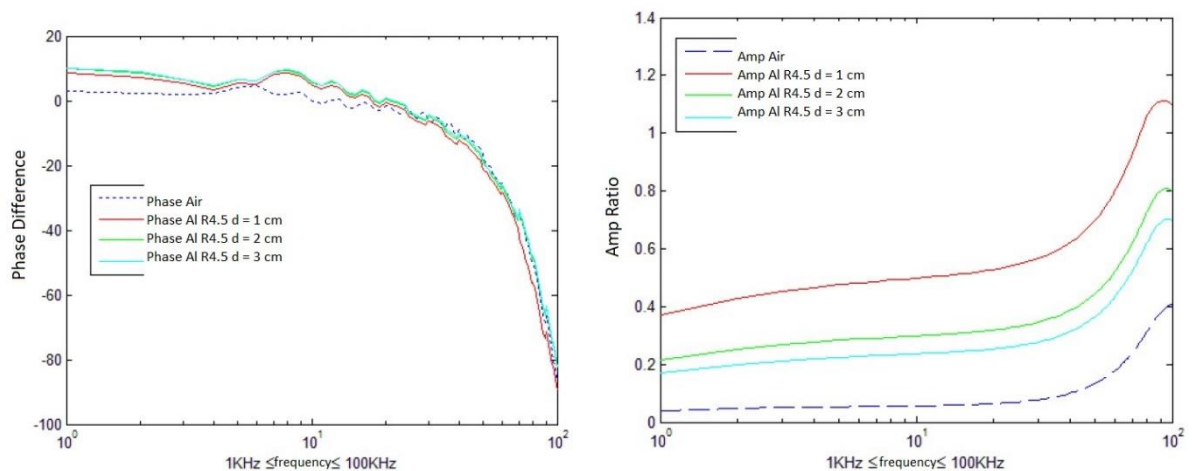
Figure 5.12 : R=4.5 cm aluminum cylinder phase difference and amplitude ratio
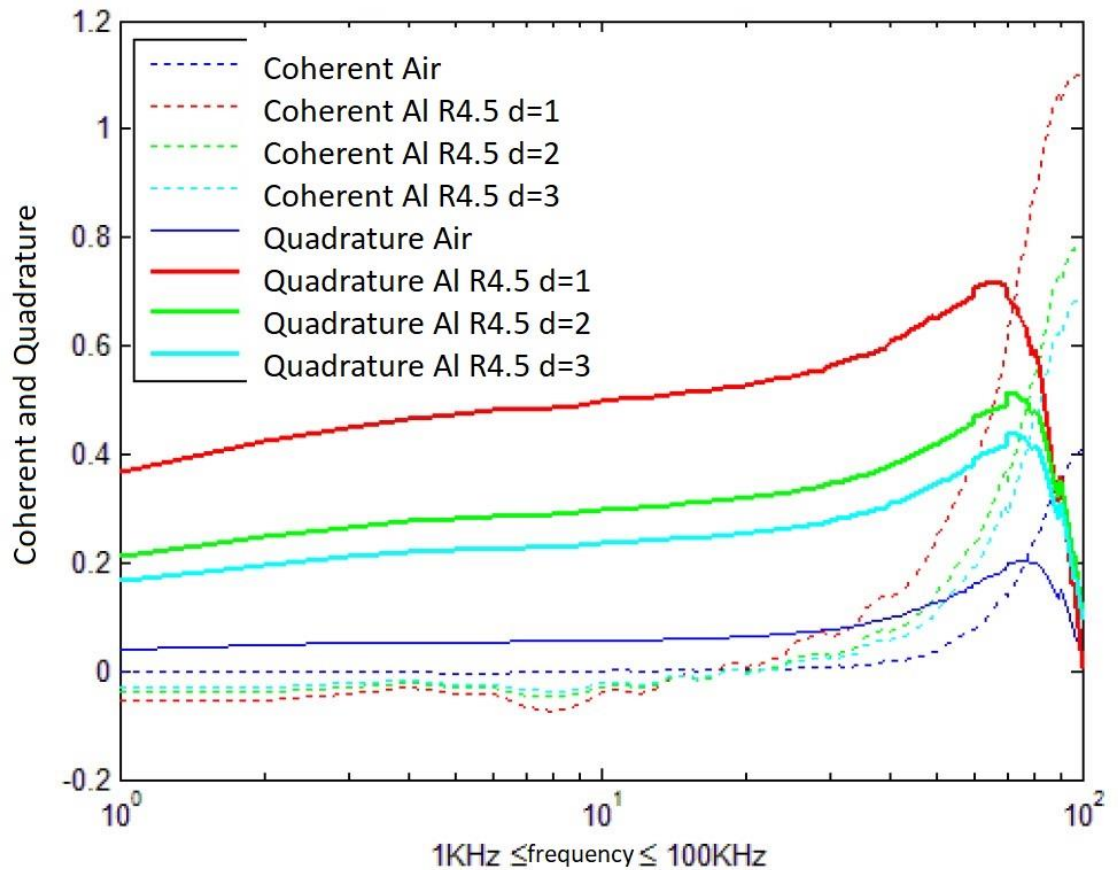
Figure 5.13 : Measurement of R=4.5 cm aluminum cylinder quadrature and coherent.

The coherent intersection frequencies of the object were measured as 17.5 kHz for d = 10 mm, 22 kHz for d = 20 mm, and 23 kHz for d = 30 mm as the object approaches the coil. As can be seen, two aluminum cylinders of different diameters gave similar results. Phase differences are also similar. Amplitude ratios are higher for 45mm diameter aluminum. By looking at this, it can be understood that the object is bigger. However, its position (horizontal-vertical) relative to the coils is important. Results were taken in the same position.

5.7.3 Results of 8 cm diameter cylindrical iron

The measurement results are given in Figure 5.14 and Figure 5.15. Iron is a ferromagnetic material and $\mu_r \gg 1$. As expected from the measurement results, the phase difference angles are much higher than in the idle state. With this feature, aluminum and iron can be distinguished easily.
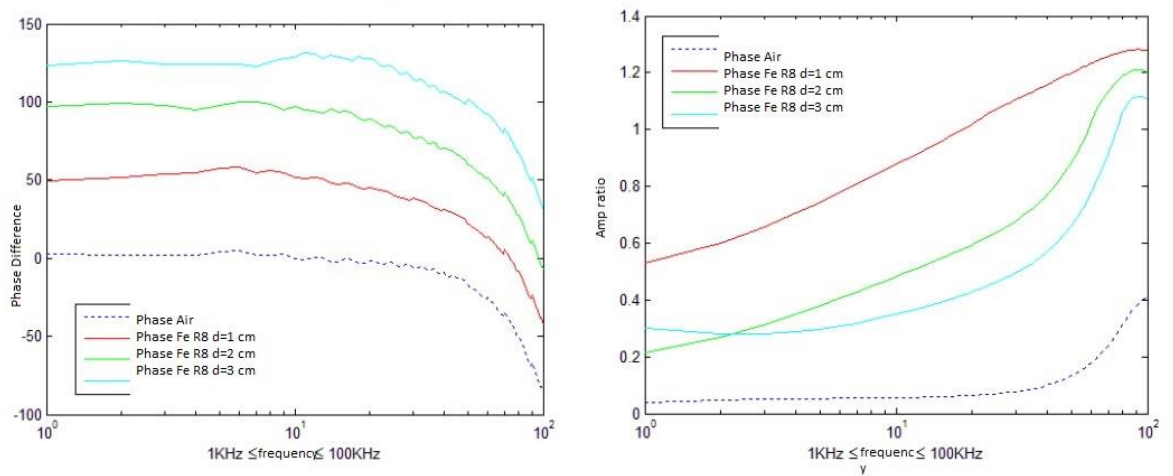
Figure 5.14 : R=8 cm iron cylinder phase difference and amplitude ratio.

Amplitude values are expected to increase as the object gets closer to the coil. In the electromagnetic theoretical analysis, while the amplitude ratio is higher at low frequencies, it decreases with the frequency. It starts to increase again depending on the magnetic permeability μ_r. This was not seen for the iron cylinder in the measurements taken. The phase difference angle has changed depending on the distance of the object. The phase difference decreases as the transceiver gets closer to the coil.
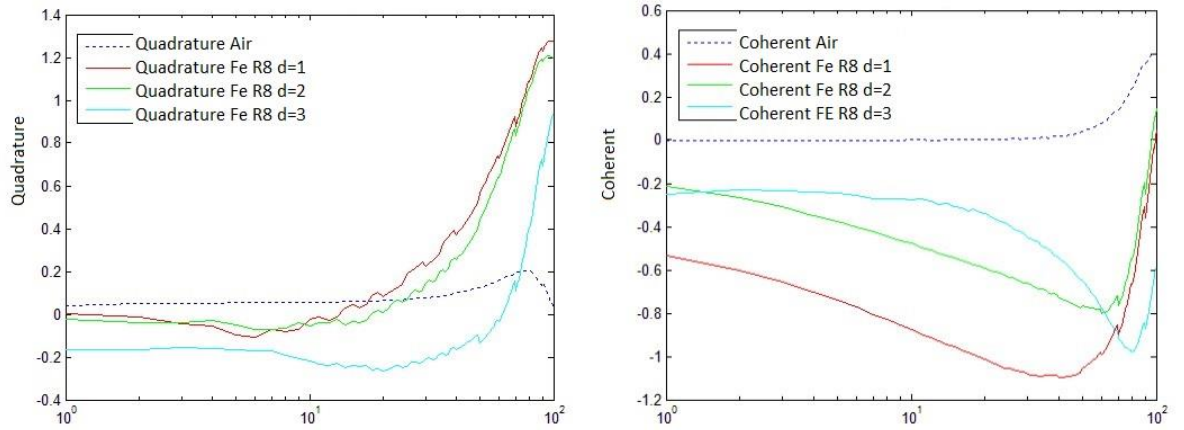
Figure 5.15 : Measurement of R=8 cm iron cylinder, quadrature and coherent.

Coherent values are below zero. This is the salient feature of ferromagnetic materials.
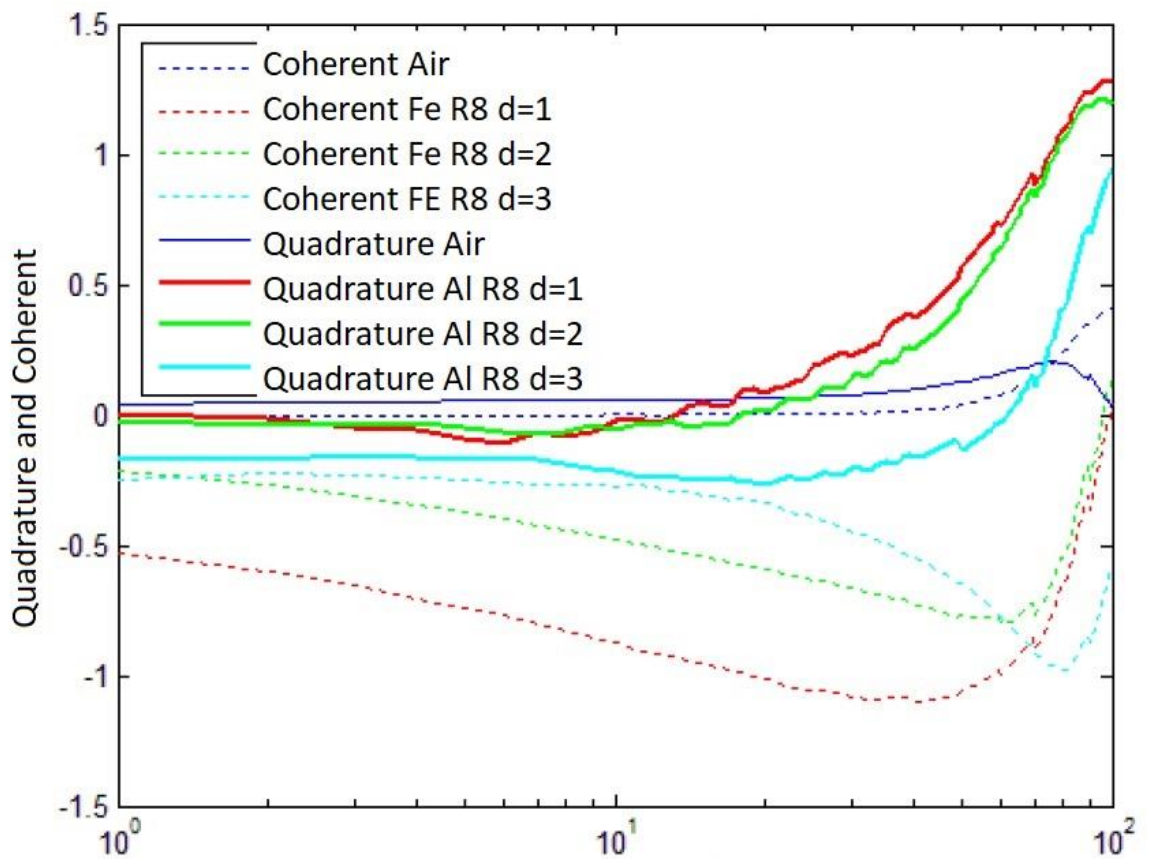
Figure 5.16 : Comparison of R=8 cm iron cylinder, quadrature and coherent measurement.

5.7.4 Results of comparing different objects

The phase and amplitude measurement results of 4 different objects are given in Figure 5.17. The objects are 50 cents, iron bars, R = 8 cm iron cylinder and R = 4.5 cm aluminum cylinder. Frequency characteristics were investigated by taking measurements from 4 objects with different dimensions and magnetic properties.
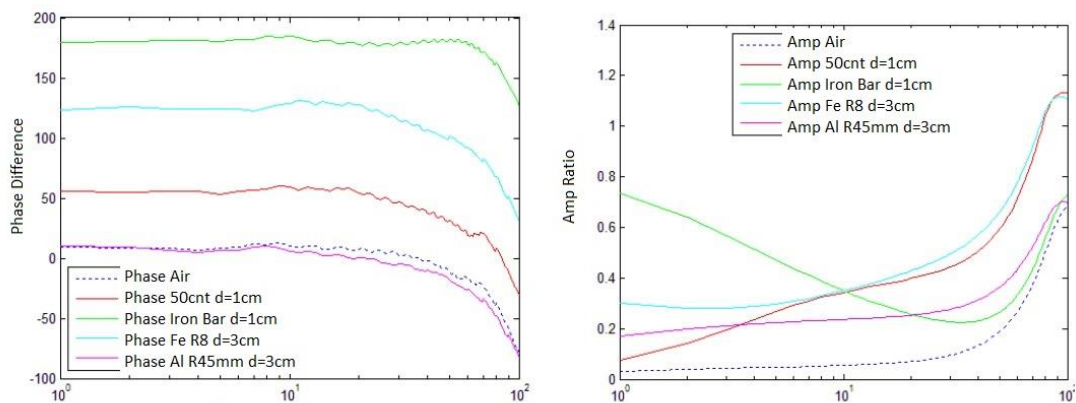
Figure 5.17 : Phase difference and amplitude ratio of four objects.

The 50 cent coin material is an alloy of iron, chromium and nickel. It is ferromagnetic material. For 50 cents, iron bars and iron cylinders, the phase difference is greater than that of non-ferromagnetic aluminum and can be distinguished. The iron rod amplitude ratio is in line with the theoretical analysis results. It was expected that the iron cylinder would have a decreasing amplitude value and then increasing again. The reason why the same result cannot be obtained from the iron cylinder may be due to its large diameter.

The amplitude ratios of 50 cent cylinder are approximately close to each other. Two different materials are separated by phase difference. For 50 cent coin, the phase difference is 55 k at 3 kHz. For an iron cylinder, it is 124.1˚. The phase difference of the two objects is 69 ˚ during the whole operating frequency. Objects can be classified using these data. Quadrature and coherent measurement results are given in Figure 5.18 and Figure 5.19.
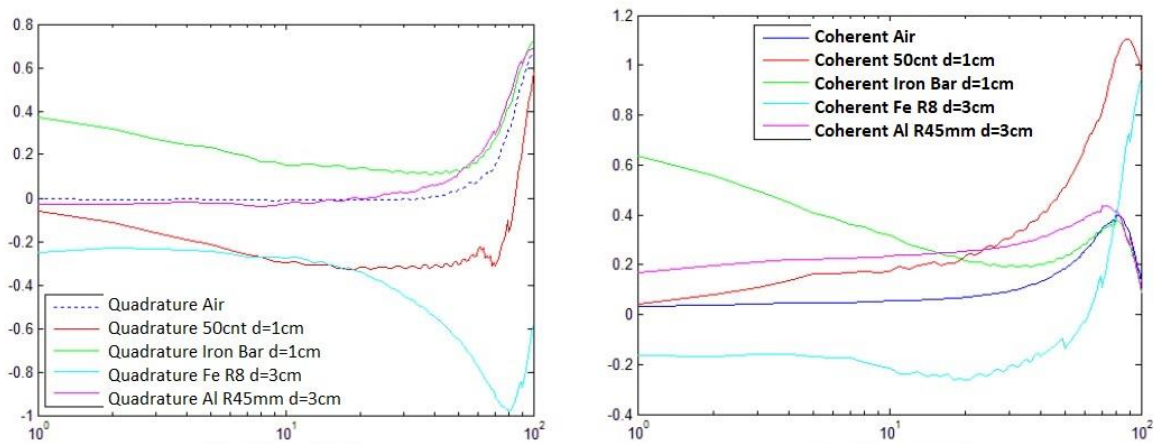
Figure 5.18 : Quadrature and coherent measurement of four objects.

With 50 cents, the coherent-frequency characteristics of the iron cylinder are similar. In shape, it can be caused by the fact that both are cylinders.
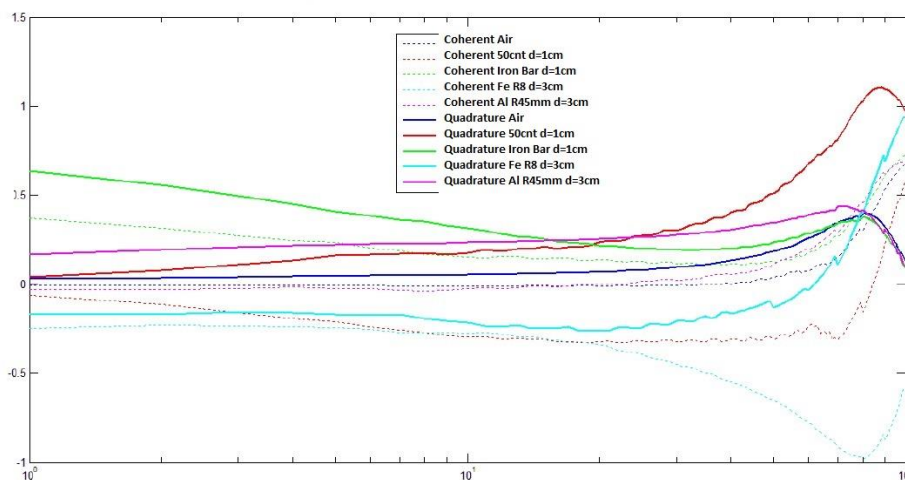
Figure 5.19 : Comparison of R=8 cm iron cylinder, quadrature and coherent measurement.

5.7.5 Comparison results of mines and other objects

The expectations of users from metal detectors are that they can detect metallic objects and classify the objects and not detect unwanted metallic objects. In this test scenario, the characteristics of mines and other objects in the frequency domain have been extracted. The measurement results are given in Figure 5.20 and Figure 5.21. 50 guns, PMN anti-personnel mines, TS50 anti-personnel mines and R = 4.5 cm aluminum cylinder were used as test objects.
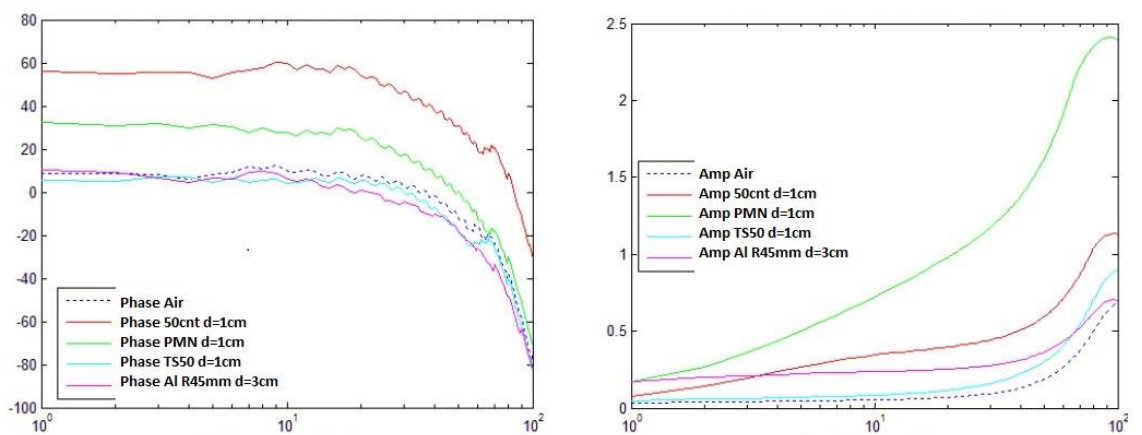
Figure 5.20 : Phase difference and amplitude ratio of mines and other objects.

When we look at the phase data, we can see that the igniter part inside the PMN mine is made of ferromagnetic material. Phase shift in TS-50 and aluminum disc is very small as expected. Phase information is insufficient in distinguishing two objects. At 66 kHz, the amplitude ratio is at the same level, but the amplitude ratio gives different results in the entire frequency band.
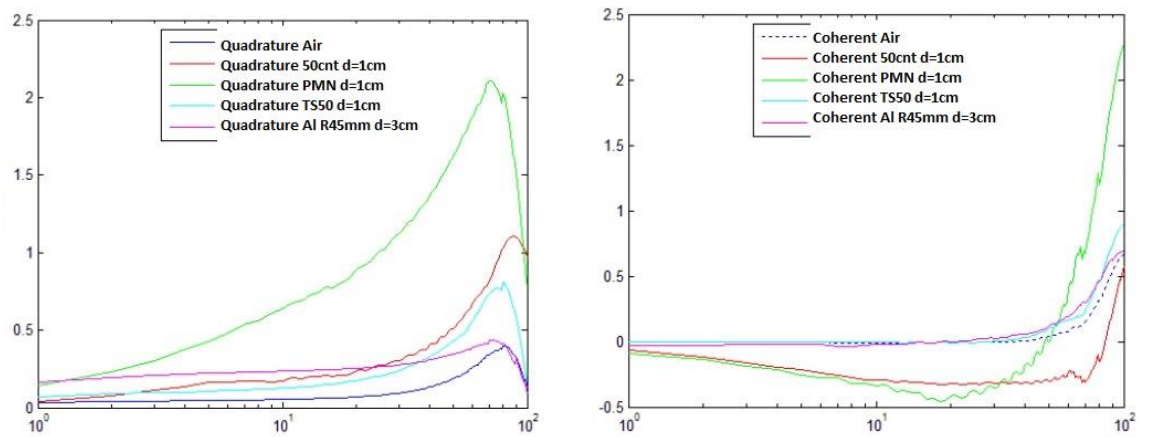
Figure 5.21: Quadrature and coherent measurement of mines and other objects.

The difference between TS-50 and aluminum cylinder is clearly seen in the rectangular part of the sign taken from the objects. The results of the perpendicular portion of the 50 cents and PMN anti-personnel mines show that it is possible to distinguish the two objects. The peaks of the orthogonal values were examined. The results are presented in Table 5.1. The peak of the air and 50 cents objects are at the same frequency. It has been observed that there is no distinct peak frequency for ferromagnetic and non-ferromagnetic objects.

Air	PMN	TS-50	50 cent	R=4.5 cm Al cylinder
80 kHz	70 kHz	82 kHz	80 kHz	71 kHz
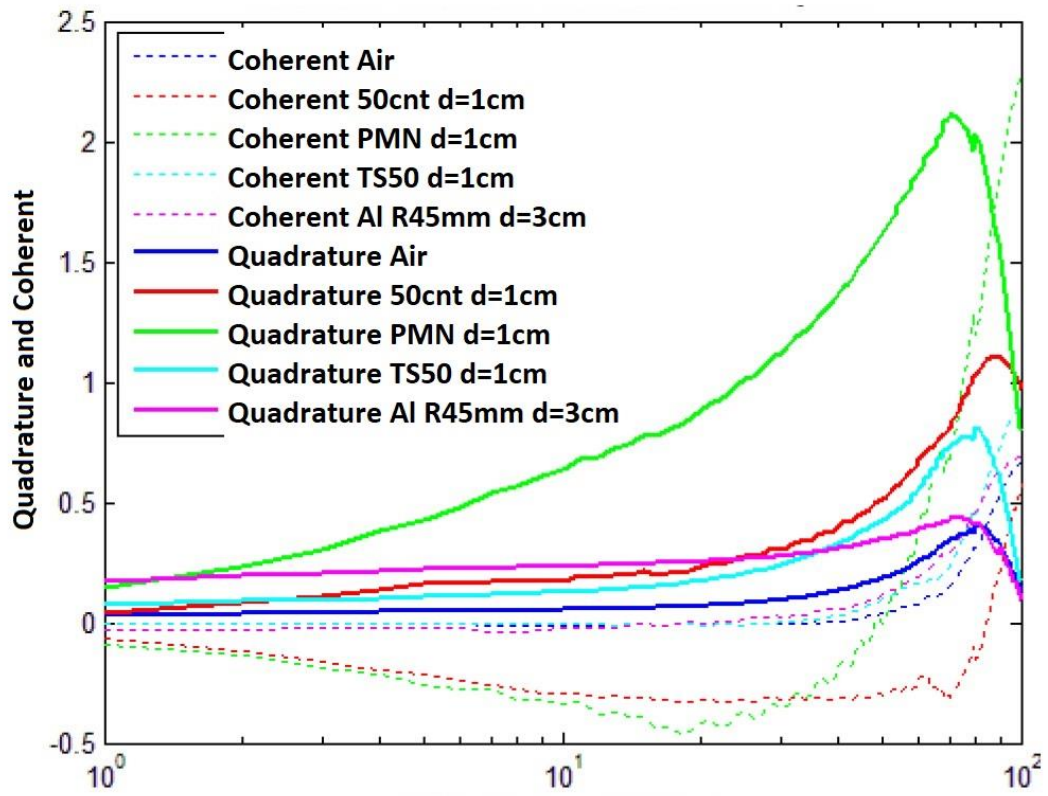
Figure 5.22 : Comparison of quadrature and coherent measurement of mines and other objects.

6. CONCLUSIONS AND RECOMMENDATIONS

In the thesis, a multiple metal detector operating in the range of 1 kHz - 100 kHz, with 100 different frequencies at 1 kHz intervals was designed. It has been measured and analyzed under laboratory conditions. By comparing the measurement results with the result of theoretical analysis, it has been observed that the system works in accordance with the electromagnetic induction model.

In the hardware part, coil values suitable for operation in the range of 1 kHz-100 kHz are calculated. Operating frequency is the lower linear part of the resonant frequency of the coil, unlike metal detectors operating at a single frequency. It has been observed that if the coil values are not selected appropriately and the quality factor Q is high, it cannot be operated efficiently at the entire operating frequency. It has been seen in the measurement results that the inductance value is less than 8 mH, and it is not suitable for broadband operation, especially around 500 µH. The Double-D coil was prepared by winding 90 turns of copper wire for the receiver coil and 80 turns of copper wire for the transmitter coil according to the calculated inductance value. Coils are protected from external EM interference by wrapping them in metallic fabric. In addition, capacitive effect between the surface and the coil is prevented. The change of the inductance of the coils with the capacitive effect causes a false alarm. A low-noise amplifier has been selected for the receiver circuit to have a high signal-to-noise ratio. The 33 dB received signal is amplified. The gain of the amplifier is set at a level that does not saturate the amplifier when the large metallic object approaches.

In the study, it has been seen that it is possible to classify different objects according to their phase responses. In addition, it was observed that the real and imaginary data of the objects that caused the wrong detection differ. By using these data, the false alarm rate that degrades the performance of metal detectors can be reduced. When the phase responses were examined, it was

seen that there was a distinctive difference between ferromagnetic and non-ferromagnetic objects. Especially the phase difference occurring between 1 kHz-20 kHz is more pronounced. As the frequency goes to 100 kHz, the phase difference approaches zero as in non-ferromagnetic objects. This is the reason why 1 kHz-20 kHz is generally used in commercial single frequency products. In metals such as non-ferromagnetic aluminum, the phase difference does not change with the height of the object, but in ferromagnetic metals such as iron, the phase difference is dependent on the height. This difference has also been observed in Förster Minex detector analyzes [9]. It has been observed that the study conducted works similarly with both the electromagnetic induction model and other commercial products.

As a result of the thesis, the working logic of the multi-frequency metal detector and the interpretation of the signals coming from the objects was acquired. There has been an important accumulation of knowledge for future studies. In order to get more realistic data in the next studies, the analyzes will be made by burying the objects in soils of different properties. The characteristics of metallic objects in the soil in the frequency domain will be inferred. Its effect on soil compensation will be investigated.

List of Sources

[1] Turk, A., Hocaoglu, A. and Vertiy, A. (2011). Subsurface sensing. Hoboken, N.J.: Wiley.

[2] Aksoy, S. (2014). Advanced Metal Detectors Webbook. Retrieved on: 15.12.2014, address: http://anibal.gyte.edu.tr/dosya/102/~saksoy/Metal%20Detectors/Advanced%20Metal%20Detectors%20-%20Book.html

[3] Haines, N. (1986). Research techniques in nondestructive testing volume VIII. NDT International, 19(6), p. 419-420.

[4] Svatos, J., Vedral, J., and Fexa, P. (2011). Metal Detector Excited By Frequency-Swept Signal. metrol. Meas. syst. , vol. XVIII, no. 1, p. 57–68.

[5] Svatos, J., and Vedral, J. (2012). The Usage of Frequency Swept Signals for Metal Detection. IEEE TRANSACTIONS ON MAGNETICS, VOL. 48, NO. 4, p. 1501-1504, April.

[6] Gao Ping Gao, Collins, L., Garber, P., Geng, N., and Carin, L. (2000). Classification of landmine-like metal targets using wideband electromagnetic induction. IEEE Trans. geosci Remote Sensing, 38(3), 1352-1361.

[7] Lahrech, A., Zaoui, A., Benyoubi, F., and Sakoub, A. (2013). Modeling of inductive metal detector with swept frequency excitation. 2013 International Conference On Electromagnetics In Advanced Applications (ICEAA).

[8] Gaffney, C. (2008). Detecting trends in the prediction of the buried past: A review of geophysical techniques in archaeology. Archaeometry, 50(2), 313-336.

[9] Bruschini, C. (2002). A Multidisciplinary Analysis of Frequency Domain Metal Detectors for Humanitarian Demining (PhD thesis). Brussels, Belgium: Vrije Universiteit Brussels.

[10] Ripka, P. (2001). Magnetic sensors and magnetometers. Boston: Artech House.

[11] Dehmel, G. (1989). Magnetic Field Sensors: Induction Coil (Search Coil) Sensors. Weinheim, Germany: Sensors, p. 205-253.

[12] Telford, W. (1976). Applied geophysics. London: Cambridge University Press, Cambridge, p. 362-365.

[13] McFee, J.E. (1989). Electromagnetic Remote Sensing: Low Frequency Electromagnetics, Defense Research Establishment Suffield, Ralston, Alberta, Canada, Suffield Special Publication No.124 (report DRES-SP-124), January 1989.

[14] Kaufman, A., Eaton, P., and Kaufman, A. (2001). The theory of inductive prospecting. Amsterdam: Elsevier Science B.V.

[15] Riggs, L., Mooney, J., and Lawrence, D. (2001). Identification of metallic mine-like objects using low frequency magnetic fields. IEEE Trans. geosci Remote Sensing, 39(1), 56-66.

[16] Carin, L., Won, I., Keiswetter, D. (1999). Wideband frequency- and time-domain EMI for mine detection, Proc. SPIE, 3710, 14-25.

[17] Shubitidze, F., O'Neill, K., Sun, K., and Shamatava, I. (2002). Application of broadband EMI responses to infer buried object's aspect ratio. IEEE International Geoscience And Remote Sensing Symposium. (IGARSS '02), 3, 1542-1545, June 24-28, Toronto, CANADA.

[18] Grant, F., & West, G. (1965). Interpretation theory in applied geophysics. New York: McGraw Hill.

[19] Ozakin, M.B. (2011). Modeling of a Metal Detector in Three Dimensional Cartesian Coordinates in Quasi-Static Time Space with Finite Difference Method (master's thesis). Gebze, Turkey: Gebze Institute of Technology.

[20] Wheeler, H. (1982). Inductance Formulas for Circular and Square Coils, Proceedings of the IEEE, Vol. 70, no. 12, December, 1449-1450.

[21] Vallon Metal Detectors. (2014). Vallon Mine Detection Multi-Sensor Systems VMM3. Received: 15.12.2014, address: http://www.vallon.de/products.lasso?a=mine-detection&b=3

[22] TUBITAK. (2014). ETMTS-2 Handheld Mine Detection System . Retrieved on: 15.12.2014., Address: http://bilgem.tubitak.gov.tr/tr/icerik/etmts-2-elde-tasinresim-mayin-tespit-sistemi.

[23] Garrett Metal Detectors (n.d.). Garrett Sport Division, Hobby Gold Detectors. Retrieved 12/15/2014, address: http://www.garrett.com/hbby_at_gold_main_international.aspx

[24] Secuda Body Search Detectors. (n.d.). Secuda Security Systems. Retrieved on 15.12.2014, address: http://www.secuda.com.tr/secuda-crx-guvenlik-el-ust-arama-dedektoru.

[25] Candy, B. (2014). Minelab Metal Detector Technical Notes. Retrieved 12/15/2014, address: http:// ww.minelab.com/emea/consumer/knowledge-base/minelabtechnologies.

[26] Bies, L. (2014). Easy to build pulse induction metal detector with DSP. Lammertbies.nl., Retrieved 12/15/2014, address: http://www.lammertbies.nl/electronics/PI_metal_detector.html.

[27] Mine Detection Systems. (2014). Introduction - Schiebel. Retrieved 12.12.2014, address: https://www.schiebel.net/Products/MineDetectionSystems/ ATMID.aspx.

[28] Ni.com. (2014). NI LabVIEW National Instruments. Retrieved 12.12.2014, address http://www.ni.com/labview.